Title
Impulse response functions of terrestrial carbon cycle models: method and application

Journal
Global Change Biology, 5(4)

ISSN
1354-1013

Authors
Thompson, Matthew V
Randerson, James T

Publication Date
1999-04-01

DOI
10.1046/j.1365-2486.1999.00235.x

Global Change Biology (1999) **5,** 371–394

Impulse response functions of terrestrial carbon cycle models: method and application

MATTHEW V. THOMPSON* and JAMES T. RANDERSON†
*Department of Organismic and Evolutionary Biology, Harvard University, 16 Divinity Avenue, Cambridge, MA, 02138, USA, †Carnegie Institution of Washington, Department of Plant Biology, 260 Panama Street and, Stanford University, Department of Biological Sciences, Stanford, CA, 94305, USA

Abstract

To provide a common currency for model comparison, validation and manipulation, we suggest and describe the use of *impulse response functions*, a concept well-developed in other fields, but only partially developed for use in terrestrial carbon cycle modelling. In this paper, we describe the derivation of impulse response functions, and then examine (i) the dynamics of a simple five-box biosphere carbon model; (ii) the dynamics of the CASA biosphere model, a spatially explicit NPP and soil carbon biogeochemistry model; and (iii) various diagnostics of the two models, including the latitudinal distribution of mean age, mean residence time and turnover time. We also (i) deconvolve the past history of terrestrial NPP from an estimate of past carbon sequestration using a derived impulse response function to test the performance of impulse response functions during periods of historical climate change; (ii) convolve impulse response functions from both the simple five-box model and the CASA model against a historical record of atmospheric $\delta^{13}C$ to estimate the size of the terrestrial ^{13}C isotopic disequilibrium; and (iii) convolve the same impulse response functions against a historical record of atmospheric ^{14}C to estimate the ^{14}C content and isotopic disequilibrium of the terrestrial biosphere at the 1° × 1° scale. Given their utility in model comparison, and the fact that they facilitate a number of numerical calculations that are difficult to perform with the complex carbon turnover models from which they are derived, we strongly urge the inclusion of impulse response functions as a diagnostic of the perturbation response of terrestrial carbon cycle models.

Keywords: biogeochemistry, carbon, impulse response, isodisequilibrium, sink, turnover

Received 18September 1997; revised version received 25 March and accepted 3 June 1998

Introduction

The global carbon budget has changed significantly due to anthropogenic increases in atmospheric carbon dioxide (Keeling *et al.* 1989), and many suspect this increase may have wide-ranging effects on global climate as well as on basic terrestrial physiological and hydrological processes (Schimel *et al.* 1995). But the magnitude of the potential change is uncertain (Moore & Braswell 1994; Sarmiento *et al.* 1995; Joos *et al.* 1996) as well as confounded by uncertainties in the scope of human activity (Houghton & Meira Filho 1995; Schimel 1995). A major question is whether the oceans or the terrestrial biosphere can mediate the recent increases in atmospheric carbon dioxide by increasing their carbon sequestration rates.

Correspondence: Matthew Thompson, tel + 1/617-496-3580, fax + 1/617-496-5854, e-mail mthompson@oeb.harvard.edu

There is considerable evidence now that the terrestrial biosphere is, indeed, a significant sink of atmospheric carbon, as seen in analyses of atmospheric and ocean data (Tans *et al.* 1990; Ciais *et al.* 1995a; Ciais *et al.* 1995b), as well as in studies of the sensitivity of production to increased atmospheric CO_2 (Farquhar & Sharkey 1982; Farquhar & Wong 1987; Luo & Mooney 1995; Wullschleger *et al.* 1995; Amthor & Koch 1996; Luo *et al.* 1996) or nitrogen availability (Field & Mooney 1986; McGuire *et al.* 1992; McMurtrie & Wang 1993; Townsend *et al.* 1996; Holland *et al.* 1997; Vitousek *et al.* 1997a; Vitousek *et al.* 1997b). If production is actually increasing, it may lead to significant increases in carbon storage if the turnover of carbon is sufficiently slow (Taylor & Lloyd 1992; Friedlingstein *et al.* 1995; Lloyd & Farquhar 1996; Thompson *et al.* 1996; Townsend *et al.* 1996). The

potential of a given ecosystem to maintain a significant carbon sink is given by the system's *sink potential*, or the product of NPP and the turnover time of the system, $P\tau$ (Taylor & Lloyd 1992; Thompson *et al.* 1996), where P is production and τ is the turnover time.

Carbon turnover, however, unlike photosynthesis, is less well understood, due largely to its hidden, complex and heterogeneous nature (see review by Stevenson 1994). Soil chemical transformations are controlled by many things, including temperature, texture, moisture, biota, relief, and nutrient availability (Jenny 1980). Some soil carbon models, such as CENTURY (Parton & Scurlock JMO Ojima 1993; Schimel *et al.* 1994), Rothamsted (Jenkinson 1990; Jenkinson *et al.* 1991), Biome-BGC (Running & Coughlan 1988; Running 1990; Running & Hunt 1993) and FBM (Kindermann & Lüdeke MKB Badeck 1993; Lüdeke & Otto 1994; Lüdeke & Otto 1995), have tackled these controls. For the sake of convenience, these models consign various classes of carbon compounds to a number of plant, detrital and soil carbon pools. There is little support for one model pool structure over another, and in many cases, this has inspired simplification of the models, reducing the controls to soil texture and climate (Schimel *et al.* 1994).

The impulse response approach

An impulse response function, defined as the system response to an impulse as a function of time since the impulse, can be derived from any model that is sufficiently linear and time-invariant (Nir & Lewis 1975; Lewis & Nir 1978). The rudiments of impulse response functions can be found in some of the very earliest literature analysing the carbon cycle, where the idea was to incorporate terrestrial functions into coherent, integrated and dynamic models of the entire global carbon cycle (Eriksson & Welander 1956; Eriksson 1971; Bolin & Rodhe 1973; Bolin 1975). They are also successful in describing the movement of tracers in atmospheric and ocean models (Siegenthaler & Oeschger 1978; Maier-Reimer & Hasselmann 1987; Sarmiento *et al.* 1992; Joos *et al.* 1996), and they have already been applied, at least in principle, to terrestrial carbon cycle models (Emanuel *et al.* 1981; Emanuel *et al.* 1984; Moore & Bolin 1986/1987; Siegenthaler & Oeschger 1987; Moore & Braswell 1994; Joos *et al.* 1996).

Impulse response functions are powerful analytical tools. By convolving them against historical records of model tracer input (such as the concentration of atmospheric $^{13}CO_2$ and $^{14}CO_2$, or against terrestrial NPP), one can efficiently calculate the isotopic disequilibria of ^{13}C or ^{14}C in the terrestrial biosphere (Enting *et al.* 1993; Enting *et al.* 1995; Fung *et al.* 1997), the ^{13}C and ^{14}C contents of various soil compartments (Balesdent 1987; Trumbore *et al.* 1995), or the controlling relationship between changes in NPP and the terrestrial carbon sink (Taylor & Lloyd 1992; Friedlingstein *et al.* 1995; Thompson *et al.* 1996; Townsend *et al.* 1996). Impulse response functions are not widely used, and they have not yet been applied to spatially resolved, complex models of terrestrial carbon turnover. Nevertheless, their potential utility in studies that explore the role of the terrestrial biosphere in the global carbon cycle is enormous (Joos *et al.* 1996).

This study

By demonstrating and refining this method we hope to clarify its use and encourage comparison and validation of complex carbon turnover models via their impulse response functions. We present the method and demonstrate its usefulness with respect to (i) the dynamics and diagnostics of continuous and discrete pool-based terrestrial carbon cycle models, (ii) the relative performance of an impulse response function compared to the model from which it was derived, and (iii) the utility of impulse response functions in calculating the reciprocal impacts of changes in atmospheric ^{13}C and ^{14}C on plant and soil isotopic content, as well as changes in biosphere function on atmospheric isotopic content.

Methods

Impulse response functions

Definitions. In practice, we find that different fractions of carbon leave the system at different times. The time it takes for a parcel of carbon to traverse a system is called its *transit time* or *mean residence time*, τ. Different parcels of carbon have different transit times. Each parcel also has an age, T, which is the time the carbon has spent in the system since sequestration via photosynthesis.

The steady-state distribution of carbon leaving the system as a function of transit time is called the *impulse response* of the system, $\Phi(\tau)$. The integral of $\Phi(\tau)$, with respect to τ, gives the total flux, Φ_T, into and out of the system at steady state:

$$\Phi_T = \int_0^\infty \Phi(\tau)\, d\tau . \qquad (1)$$

Note that Φ_T does not vary with time, since $\Phi(\tau)$ is a steady state function. $\Phi(\tau)$ normalized by Φ_T is the probability density function of transit times, τ, in the system:

$$\phi(\tau) = \frac{\Phi(\tau)}{\Phi_T}; \int_0^\infty \phi(\tau)\, d\tau = 1 \qquad (2)$$

$\phi(\tau)$ is also called Green's function, or kernel function,

and is analogous to the 'unit hydrograph' used in groundwater precipitation response functions. $\phi(\tau)$ can also be defined as (Lewis & Nir 1978): (i) the probability density function of transit times in the parcels of carbon entering the system, (ii) the outflow response of the whole system (in this case, the terrestrial biosphere) to an instantaneous input such as the Dirac delta function, or (iii) a weighting function describing the relative contribution of different inflows at times $(t - \tau)$ to the present outflow at time t. Inflow, in the case of the terrestrial biosphere, is gross (or net) primary production, while outflow is ecosystem (or heterotrophic) respiration. The first moment of $\phi(\tau)$ with respect to τ is the mean transit time of carbon, $\bar{\tau}$:

$$\bar{\tau} = \int_0^\infty \tau\phi(\tau)\, d\tau \tag{3}$$

or, in other words, the average time required for a given parcel of carbon to traverse the biosphere from sequestration to eventual release through respiration.

Each parcel of carbon in the biosphere has an associated age. The distribution of carbon in the terrestrial biosphere with respect to that age is the *storage response* of the system, $\Psi(T)$, and can be alternatively defined as a weighting function giving the contribution of carbon sequestered at time $(t - T)$ to the carbon presently stored in the system at time t. This function can be integrated with respect to T to give the total carbon storage of the terrestrial biosphere Ψ_T at steady state:

$$\Psi_T = \int_0^\infty \Psi(T)\, dT \tag{4}$$

$\Psi(T)$ normalized with respect to Ψ_T is the probability density function of carbon storage with respect to T:

$$\psi(T) = \frac{\Psi(T)}{\Psi_T}; \int_0^\infty \psi(T)\, dT = 1 \tag{5}$$

and the first moment of $\psi(T)$ with respect to T is the mean age, $\overline{T}$, of carbon currently present in the biosphere:

$$\overline{T} = \int_0^\infty T\ \psi(T)\, dT \tag{6}$$

$\overline{T}$ and $\bar{\tau}$ are equivalent when $\phi(\tau)$ has an exponential form; that is, in a single- reservoir, first- order turnover model, the mean age and mean transit time are the same (Bolin & Rodhe 1973).

An additional parameter, definable using terms described above, is the turnover time τ_o; it is usually expressed as the ratio of total carbon storage in the system to flux through the system:

$$\tau_o = \frac{\Psi_T}{\Phi_T}. \tag{7}$$

Bolin & Rodhe (1973) showed that $\bar{\tau}$ and τ_o are equivalent at steady state. They subdivide steady-state systems into three different categories (Bolin & Rodhe 1973; Rodhe 1992): (i) $\overline{T} < \bar{\tau} = \tau_o$, in which carbon spends some finite time in the system before any appreciable fraction is respired (such as in the human population, where mean age may be around 30 but life expectancy is 70); (ii) $\overline{T} = \bar{\tau} = \tau_o$, in which carbon is well – mixed and the probability of respiration remains constant irrespective of physical or temporal position within the system; and (iii) $\overline{T} > \bar{\tau} = \tau_o$, in which the probability of respiration declines the longer the carbon spends in the system (this is the situation most representative of that found in terrestrial ecosystems).

The age of each parcel, T, is the time since entering the system, while the transit time, τ, is the time required for a particle to traverse the system, irrespective of where it is found in the system. As soon as the particle departs the system, $T = \tau$. Making the distinction between the two is necessary for the development of the concepts presented here, but for practical purposes, it is necessary to switch to the sole use of τ for both τ and T. τ now represents the time since the particle entered the system: $\phi(\tau)$ is the fraction of the initial impulse departing the system at time τ, and $\psi(\tau)$ is the fraction of the initial pulse remaining in the system at time τ after sequestration. $\overline{T}$ and $\bar{\tau}$ will still be used for the mean age and mean transit time.

Additional diagnostics. At steady state, the quotient of the impulse response function and storage response function, $k(\tau)$, describes the probability of loss from the system as a function of age:

$$k(\tau) = \frac{\Phi(\tau)}{\Psi(\tau)}. \tag{8}$$

Note the use of $\Phi(\tau)$ and $\Psi(\tau)$, rather than $\phi(\tau)$ and $\psi(\tau)$; in this case, we are interested in absolute carbon loss with respect to absolute carbon content. This function is called the *decay function*. $k(\tau)$ can be used only if the dynamics of the system do not change with time, i.e.

$$\frac{\partial k(\tau)}{\partial t} = 0\ . \tag{9}$$

Indeed, this condition must hold for all functions derived using the impulse response method. The reciprocal of $k(\tau)$, $\tau_o(\tau)$, gives the instantaneous turnover time of carbon as a function of age τ

$$\tau_o(\tau) = \frac{\Psi(\tau)}{\Phi(\tau)}. \tag{10}$$

Numerous $\Phi(\tau)$ and $\Psi(\tau)$ functions from different cells within a spatially explicit model can be used as a whole by aggregating them with an area-weighted sum:

$$\widehat{\Phi}(\tau) = \sum_{x}^{\text{all cells}} \Phi_x(\tau)\, A_x \tag{11}$$

$$\widehat{\Psi}(\tau) = \sum_{x}^{\text{all cells}} \Psi_x(\tau)\, A_x\,, \tag{12}$$

where A_x is the land area of cell x, and $\widehat{\Phi}(\tau)$ and $\widehat{\Psi}(\tau)$ are the new aggregated impulse response and storage response functions, respectively. The functions can be converted to $\widehat{\phi}(\tau)$ and $\widehat{\psi}(\tau)$ using (2) and (5).

Transformation of two models

The impulse response transformation: continuous vs. discrete. The transformation of carbon biogeochemistry models into their respective impulse response equivalents requires only that a pulse of carbon be applied to the model (e.g. through NPP, allocated to the different biomass pools) and followed through time as it is lost from the system through respiration. The fraction of the initial pulse remaining in the system after time τ is $\psi(\tau)$ while the fraction lost at time τ is $\phi(\tau)$. In transformations of models with a discrete time step, impulse response functions can be defined discretely:

$$\phi \approx \phi(\tau);\ \psi_\tau \approx \psi(\tau);\ \tau = 0, 1, 2, 3, \ldots \tag{13}$$

In some models, the dynamics of carbon turnover change seasonally, a prohibited condition if we are using a single impulse response function. In such cases, it is necessary to define discrete, aggregated impulse response and storage functions that include loss from all subannum time steps into a single function. Thus, the time step of the model is forced to be annual. One problem with these aggregations is that many processes operate at time scales smaller than that chosen for the transformation time step such that carbon may be lost during the same time step as the pulse (i.e. carbon is respired immediately after sequestration, such as through plant respiration, at $\tau = 0$). This is especially important when linking changes in assimilation rate with changes in carbon storage. Operationally, Ψ_τ is given by the carbon content of the system *before* the aggregated time step begins, and Φ_τ is given by the carbon lost *during* the aggregated time step.

Single reservoirs within larger systems. The impulse response of individual reservoirs within a system may be calculated by monitoring them individually. But the carbon balance of a single pool, with respect to transit time and age, is slightly more complex than that of the entire system.

First, the input to a single pool may be delayed since much of the carbon entering the pool may first pass through other pools, each with their own intrinsic turnover time. The input function of pool i can be defined in terms of the distribution of the carbon entering the pool with respect to its age, $P_i(\tau)$, where age is defined with respect to the time since the carbon entered the system. We define two cases, one in which all carbon enters the pool with an age $\tau = 0$, called *direct input*, and the other where there is some disperse distribution of ages, called *indirect input*.

Second, carbon may depart the pool in one of two ways, by respiration or by transfer to another pool. The first case is denoted $\Phi_r(\tau)$, or the distribution of respiratory fluxes with respect to age (where age is the time since the parcel of carbon first entered the system), and the other is $\Phi_t(\tau)$, or the distribution of transfer fluxes to other pools with respect to age. It is useful to define a third function that gives the total loss from the system as a function of age:

$$\Phi_l(\tau) = \Phi_r(\tau) + \Phi_t(\tau) \tag{14}$$

We can now write an equation for the mass balance of the reservoir as a function of τ:

$$\frac{d\,\Psi(\tau)}{d\tau} = P(\tau) - [\Phi_r(\tau) + \Phi_t(\tau)] = P(\tau) - \Phi_l(\tau) \tag{15}$$

where $d\Psi(\tau)/d\tau$ is the change in carbon content of the pool as a function of age. For individual reservoirs, we must be careful how we define the fluxes. For instance, to calculate the mean transit time of *a single reservoir*, or the time required to traverse it, we use the first moment of the change in carbon content with age, divided by the total, time-integrated loss rate of the reservoir:

$$\tau_o = \int_0^\infty \tau\, \frac{d\Psi(\tau)}{d\tau}\, d\tau \Bigg/ \int_0^\infty \Phi_l(\tau)\, d\tau\,. \tag{16}$$

For the mean age of carbon lost from the reservoir via respiration, we use:

$$\bar{\tau}_o = \int_0^\infty \tau\, \Phi_r(\tau)\, d\tau \Bigg/ \int_0^\infty \Phi_r(\tau)\, d\tau \tag{17}$$

and for the mean age of carbon in the reservoir, we use:

$$\overline{T} = \int_0^\infty \tau\, \Psi(\tau)\, d\tau \Bigg/ \int_0^\infty \Psi(\tau)\, d\tau\,. \tag{18}$$

These distinctions are important when comparing model predictions with actual data. $\phi_l(\tau)$, $\phi_r(\tau)$ and $\phi_t(\tau)$ can be derived from $\Phi_l(\tau)$, $\Phi_r(\tau)$ and $\Phi_t(\tau)$, respectively, using (2).

NPP vs. GPP. Some models use NPP as their carbon input from the atmosphere (i.e. GPP minus autotrophic respiration), while others use just GPP. The difference in

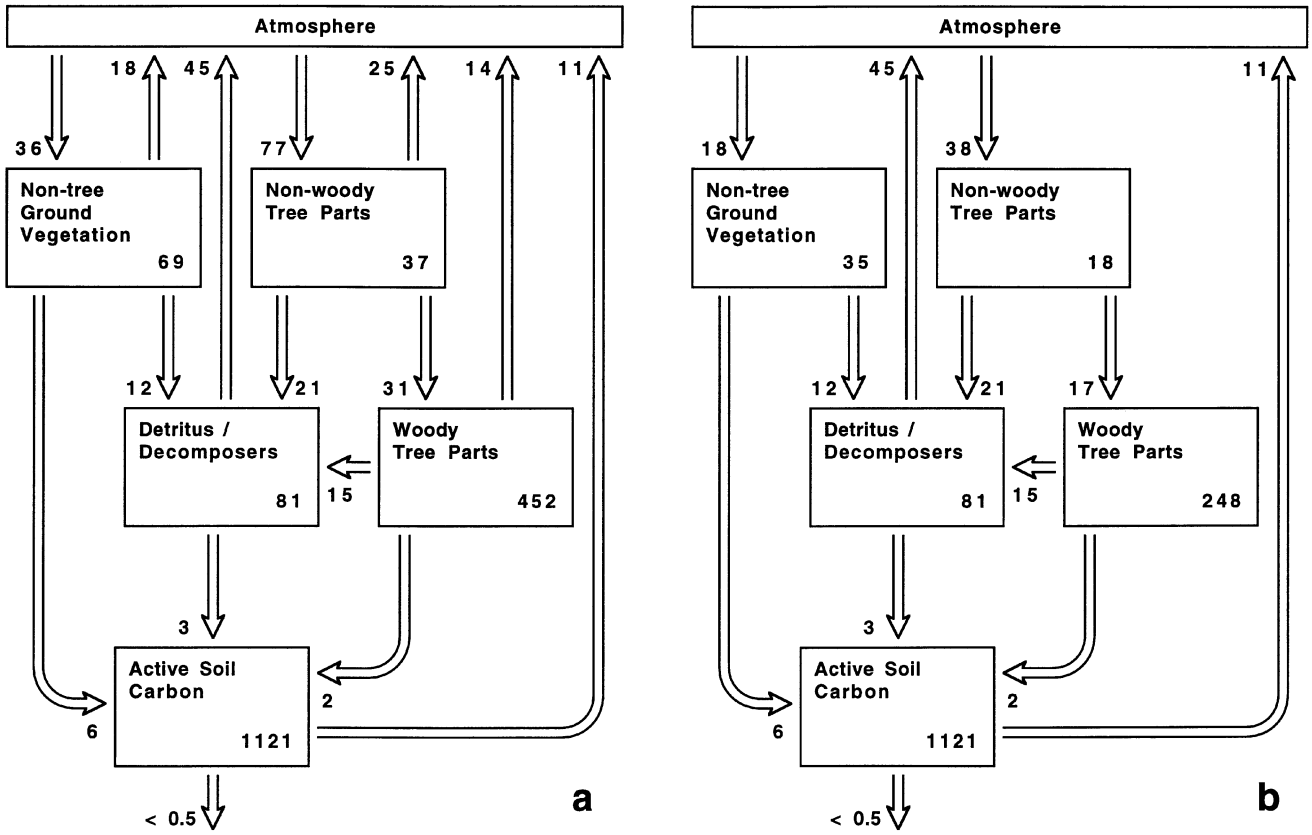

Fig. 1 The global terrestrial carbon turnover model of Emanuel *et al.* (1981). Values in boxes are the steady-state pool stocks in Pg C; values next to arrows are the annual flux rates from one pool to the next in Pg C y^{-1}. (a) The GPP-referenced version of the model where carbon is input via GPP. This model is described in eqns (A1–A3). Gross primary production (total plant assimilation or photosynthesis) is 113 Pg C y^{-1}. (b) The NPP-referenced model, derived in this paper and described in eqns (A 4-A6), with plant respiration removed and pool sizes of live biomass pools scaled to reflect overall change in input without a change in turnover time. Net primary production is 56 Pg C y^{-1}. In both models, the small flux (< 0.5) from the active soil carbon pool is ignored.

model approach has implications for the shape of the impulse response function. If plant respiration, which is composed typically of very young carbon, is included in the impulse response function (as when using GPP as the carbon input), the distribution of fluxes will be skewed toward low residence times. Models that use NPP as their input include biomass pools with their own turnover times to introduce a delay between when carbon is assimilated and when it is delivered to the soil, but these pools do not respire carbon. In the absence of a clear consensus as to whether NPP or GPP is preferable, we make a distinction between the two whenever specific models are mentioned. Models that use GPP we call *GPP-referenced* and models that use NPP, *NPP-referenced*.

A simple box model of the terrestrial biosphere. To illustrate the impulse response method, we chose the simple 5-box model of global terrestrial carbon turnover developed by Emanuel *et al.* (1981). The model (Fig. 1a) was chosen for four reasons: (i) it is simple, (ii) it is defined continuously, (iii) it is currently in use as a means of calculating the isotopic disequilibrium of ^{13}C (Enting *et al.* 1993; Francey *et al.* 1995), and (iv) it has been used as a benchmark for other models of carbon biogeochemistry (Wittenberg & Esser 1997). As such, it is an ideal tool for illustrating the impulse response concept as well as some of the pitfalls that may be encountered when using impulse response functions.

The model of Emanuel *et al.* (1981) divides terrestrial carbon storage into five reservoirs, representing nontree ground vegetation, nonwoody tree parts, woody tree parts, detritus and active soil organic matter (Fig. 1a). It is a GPP-referenced model (indicated by the inclusion of live plant biomass pools with fluxes to the atmosphere) and is defined continuously on an annual basis by the steady state reservoir contents and annual flux rates between, into and out of pools (see Appendix). We calculate the impulse response function of this model by solving the model continuously and aggregating the solutions for each reservoir into a single storage response

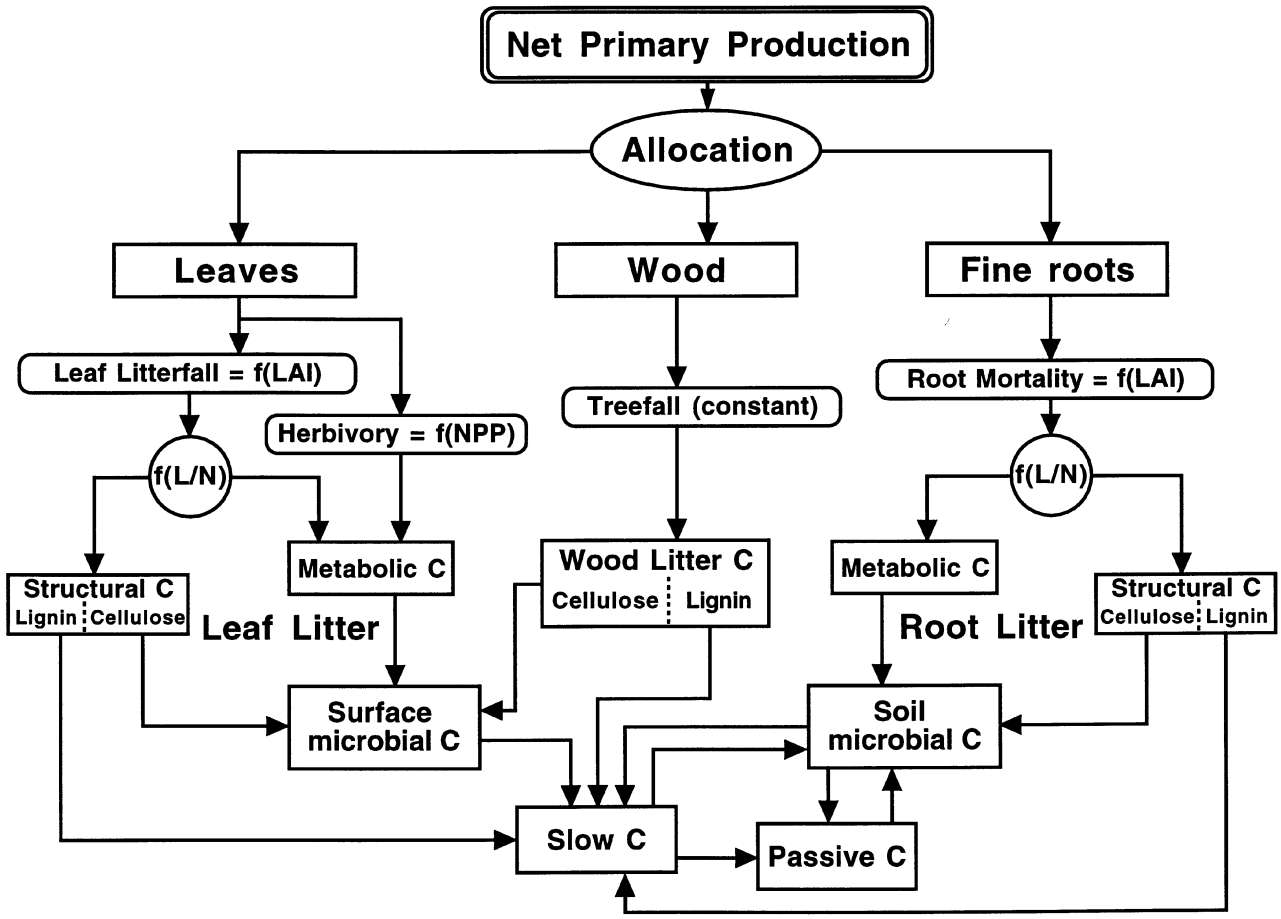

Fig. 2 The compartmentalized flow of carbon through live biomass, litter, and soil organic matter pools as described in the CASA biosphere model. For details, see Field *et al.* (1995), Randerson *et al.* (1996) and Thompson *et al.* (1996).

function, $\Psi(\tau)$. Since $\Psi(\tau)$ is defined continuously, $\Phi(\tau)$ is just the derivative of $\Psi(\tau)$. For each pool in the model, we also calculate $\psi(\tau)$, $\phi_l(\tau)$ and $\phi_r(\tau)$, as well as $\bar{\tau}$, $\overline{T}$ and τ_o. Since each reservoir decays exponentially, $\phi_l(\tau) = \psi(\tau)$, and $\bar{\tau}$ and $\overline{T}$ for each reservoir are equivalent. This is not the case for the model as a whole.

To test the difference between GPP and NPP-referenced models we convert this model into a NPP-referenced model by eliminating the plant respiration fluxes from the three biomass pools and adjusting the input fluxes accordingly, while maintaining their turnover times (Fig. 1b; see Appendix). GPP (the gross annual flux of carbon from the atmosphere to the biosphere) in this model is 113 Pg C y^{-1} (Emanuel *et al.* 1981), while NPP (under our modifications) is 56 Pg C y^{-1}, a little less than half of GPP.

The CASA biosphere model. To illustrate the impulse response concept with a more complex, iterative model, we derived impulse response functions from CASA v1.2 (Fig. 2: Field *et al.* 1995; Randerson *et al.* 1996; Thompson *et al.* 1996; Malmström *et al.* 1997), a version in all ways identical to the model version used by Thompson *et al.* (1996). The CASA model is a global, spatially resolved model operating at the 1° by 1° scale on a monthly time step. All land pixels are modelled except those that are covered by ice (i.e. vegetation classes 1–12; Defries & Townshend 1994). The NPP model is driven by air temperature and precipitation data (Shea 1986), AVHRR NDVI data from 1990 with the FASIR correction (Los *et al.* 1994) 1990 monthly surface solar irradiance (Bishop & Rossow 1991), and a 1° by 1° soil texture classification (Zobler 1986). The soil carbon model is driven with carbon from the NPP submodel of CASA, as well as by air temperature, precipitation and soil texture. Global annual NPP under CASA using these data sets is 54.9 Pg C y^{-1}. This NPP is allocated to live roots, wood and leaves at a 1:1:1 ratio (or 1:1 ratio in systems with no wood: classes 7, 10 and 12), and the different biomass pools turn over on a first-order basis, constant over each

of the vegetation classes defined by Defries & Townshend (1994). To account for the effects of herbivory on turnover, some carbon is shunted to the surface metabolic pool in proportion to annual NPP (Randerson *et al.* 1996). The biomass turnover times were derived from an analysis by Kohlmaier *et al.* (1997), but autotrophic respiration is not calculated; this is an NPP-referenced model.

Φ_τ and Ψ_τ were derived for each cell modelled by CASA on a discrete, annually aggregated basis, to a τ of 2000 years (it was not necessary, nor would it have been practical, to calculate Φ_τ or Ψ_τ to ∞ since Ψ_τ becomes vanishingly small at high τ). Using (11) and (12), individual Φ_τ's and Ψ_τ's were globally aggregated on a land area weighted basis to provide global functions analogous to the functions derived from the model of Emanuel *et al.* (1981). The Φ_τ and Ψ_τ values of three points (centred at 2.5°S 59.5°W, 54.5°N 66.5°W, and 41.5°N 99.5°W) were saved for separate analyses (see below). Ψ_τ is not defined for $\tau = 0$ since there is no carbon in the system before the pulse is applied, but this is not a concern since there is no respiration either.

Application of impulse response functions

Carbon sequestration in response to change in NPP. As Bolin *et al.* (1981) point out, with a time history of primary production and an impulse response function for the terrestrial biosphere, it is possible to calculate the time history of the sink. The gross flow of carbon from the biosphere to the atmosphere (the respiratory flow) is given by convolution integral of production against the normalized impulse response function:

$$R(t) = \int_0^\infty P(t - \tau)\ \phi(\tau)\ d\tau, \qquad (19)$$

where $P(t - \tau)$ is the rate of primary production by the biosphere at some time $(t - \tau)$. The sink rate is then the difference between the incoming and outgoing fluxes:

$$N(t) = P(t) - R(t), \qquad (20)$$

where $N(t)$ is the net flux of carbon into the system at time t. $\phi(\tau)$ can be used to calculate system respiration outside of steady state, since $P(t - \tau)$ does not need to be constant. Conversely, if $N(t)$ is prescribed from some time $t = 0$ to the present, we are given P at time $t = 0$, and P does not vary as a function of time for all $t < 0$, then we can solve for the $P(t)$ necessary to satisfy our prescribed $N(t)$, either iteratively or with a Laplace transform.

Thompson *et al.* (1996) reported that a long-term, 20% linear increase in global annual NPP over an initial value of 48.2 Pg C y^{-1} (a rate of increase of 0.1 Pg C y^{-1}) was required for the terrestrial biosphere to sequester the ≈ 90 Pg estimated to have been sequestered from 1880 to 1990 (Houghton 1995; Sarmiento *et al.* 1995). Thompson *et al.* (1996) also concluded that compared to the magnitude of the NPP-dependent changes in carbon storage, changes in climate over the last 110 years had relatively little effect on long-term changes in respiration. As such, in the absence of significant deforestation or regrowth, change in production over that period would have to have been the primary control on carbon sequestration.

To test this assumption, as well as the CASA-derived, global impulse response function, we repeated their analysis, using the same initial conditions (48.2 Pg C y^{-1} NPP and steady-state carbon storage at and before 1880) and the same estimate for the terrestrial carbon sink from the study of Houghton (1995). Since it is impossible to incorporate changing climate into impulse response functions (due to the time invariant linear dynamics assumption), this exercise will also test the extent to which changing climate influences the impulse response-derived estimate of $P(t)$.

The isodisequilibrium of ^{13}C. Changes in atmospheric ^{13}C content have been an important constraint in our estimates of the relative importance of oceans and the terrestrial biosphere as sinks for atmospheric CO_2. Fossil fuel emissions, which are depleted in ^{13}C relative to the atmosphere, have diluted the atmosphere of ^{13}C (Fig. 3), creating a mismatch between carbon sequestered by the terrestrial biosphere some time in the past and carbon being sequestered now (Keeling 1979). This mismatch is called the isodisequilibrium, D^{13} (Fung *et al.* 1997). It is formally defined as the ^{13}C flux from the atmosphere to the biosphere minus the ^{13}C flux from the biosphere to the atmosphere under conditions of steady state with respect to total carbon. It is commonly derived as the product of the gross flux of carbon between the biosphere and the atmosphere, $P(t)$, and the difference between the $\delta^{13}C$ of the atmosphere at time t and the $\delta^{13}C$ of the atmosphere at some time $(t - \bar{\tau})$, where $\bar{\tau}$ is the mean residence time of the biosphere (Tans *et al.* 1993; Ciais *et al.* 1995a; Ciais *et al.* 1995b). An important feature of the isodisequilibrium is that it increases with increasing $\bar{\tau}$.

Since the past-history of atmospheric $\delta^{13}C$ is not a linear function of time and the biosphere does not follow simple exponential decay (as in the second category of Bolin & Rodhe 1973), it is more precise to calculate D^{13} as the convolution of an impulse response function of the terrestrial biosphere against a past history of biosphere–atmospheric ^{13}C flux:

$$D^{13}(t) = -P(t)\ [\delta_A(t) + \varepsilon_{ab}(t)] + \int_0^\infty P(t - \tau)\ [\delta_A(t - \tau) + \varepsilon_{ab}(t - \tau)]\ \phi(\tau)\ d\tau, \qquad (21)$$

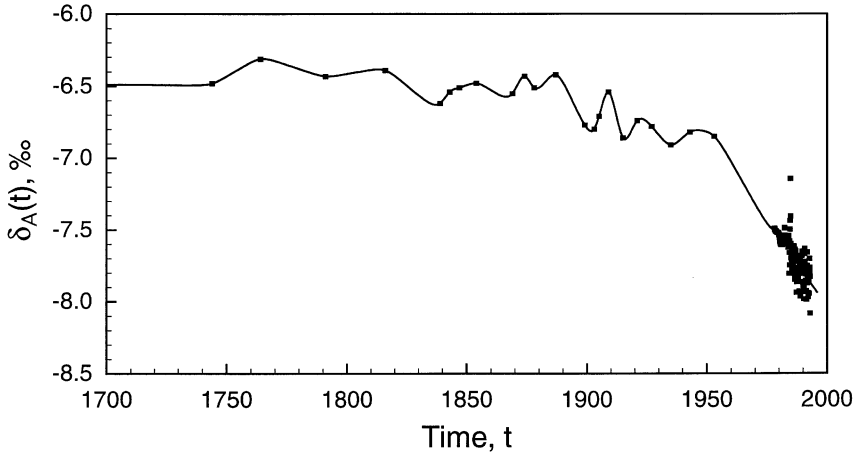

Fig. 3 Composite record of atmospheric $\delta_A(t)$ from 1700 to the present using 1700–1953 ice core data (Friedli *et al.* 1986) 1978–81 atmospheric data (Keeling *et al.* 1989), and 1982–92 aggregate atmospheric data (Francey *et al.* 1995). The connecting line is a maximally rigid spline fit of the atmospheric observations and is used as a continuous estimate of past atmospheric ^{13}C in all analyses involving ^{13}C.

where δ_A is the ^{13}C signature of the atmosphere, P is primary production (gross or net), and ε_{ab} is the photosynthetic discrimination factor (usually – 18‰ in most analyses; appropriate for C_3 plants). We assume ε_{ab} to be constant through time, so it drops out of the equation. By eqn (21), D^{13} is also a function of production. However, since D^{13} is defined as the isotopic disequilibrium when total carbon is at steady state, $P(t)$ can come out of the integral. Thus (21), for our purposes, can be rewritten:

$$D^{13}(t) = -P(t)\left[\delta_A(t) - \int_0^\infty \delta_A(t-\tau)\,\phi(\tau)\,d\tau\right]. \quad (22)$$

Isodisequilibria are often reported divided by the gross production rate:

$$\frac{D^{13}(t)}{P(t)} = \zeta^{13} = -\delta_A(t) + \int_0^\infty \delta_A(t-\tau)\,\phi(\tau)\,d\tau. \quad (23)$$

For clarity, D^{13} is the isodisequilibrium proper (a flux in units of Pg C‰ y^{-1}) and $D^{13}(t)/P(t)$ is the isodisequilibrium *forcing coefficient*, ζ. The distinction between ζ^{13} (equivalent to D_b of Fung *et al.* 1997) and D^{13} (equivalent to D_bG_b of Fung *et al.* 1997) is important: the term 'isodisequilibrium' has been used ambiguously for either one. D^{13} is an index of the impact of the biosphere on the atmospheric ^{13}C budget, while the forcing coefficient is a normalized index of the isodisequilibrium, and has meaning for the atmospheric ^{13}C only in the context of its corresponding flux.

There are presently numerous estimates for the forcing coefficient, ranging from anywhere between 0.2‰ (Tans *et al.* 1993; Ciais *et al.* 1995b) and 0.23‰ (Enting *et al.* 1993) to 0.3‰ (Fung *et al.* 1997) and 0.41‰ (Wittenberg & Esser 1997). The wide variation in these estimates (> 50%) is the result of whether the model is GPP-or NPP-referenced. The kind of variation seen in the literature translates into large uncertainty with respect to estimates of the terrestrial carbon sink. We also calculate the isodisequilibria and forcing coefficients for the different models over the period from 1977 to 1992, as well the forcing coefficient of each cell modelled by CASA in 1992, comparable with plate 2 of Fung *et al.* (1997).

Calculating the ^{14}C content of stored and respired carbon. The ^{14}C content of stored and respired carbon has been shown in recent years to be a powerful tool for directly measuring rates of carbon turnover (Trumbore 1993; Trumbore *et al.* 1995). The impulse response method, and further revisions on the method, should allow experimenters and modellers to integrate these measurements with model performance. To use impulse response functions with radiocarbon data, it is necessary to construct a past history of atmospheric ^{14}C that takes into account the effect of age. The half-life of radiocarbon, 5730 years, is what dictates this correction.

The age and $\delta^{13}C$-corrected radiocarbon content of geophysical samples is given by the following relation (Stuiver & Polach 1977):

$$\Delta = \left[\frac{A_{SN}\,e^{\gamma(1950-t)}}{A_{ON}} - 1\right]. 1000‰\,, \quad (24)$$

where A_{SN} is the activity of the sample corrected for $\delta^{13}C$, γ is 1/8267 y^{-1} (based on the 5730 years half-life), t is the year AD that the sample was created, and A_{ON} is the $\delta^{13}C$ corrected activity of the 1950 oxalic acid standard. The ^{14}C data that makes radiocarbon a useful tool for exploring plant and soil carbon dynamics is of recent origin, created in the atmosphere as a result of post WWII bomb testing. These data require no age correction. Older data, however, do require some correction assuming a constant, prebomb atmospheric Δ of 0‰. For the northern hemisphere, we use the Georgian wine data of Burcholadze *et al.* (1989) from the beginning of the bomb era to 1985; data from 1986 to 1997 are derived from an assumption of a 9.7‰ per year decrease in Δ estimated from trends in the data of Nydal & Lövseth (1996) and

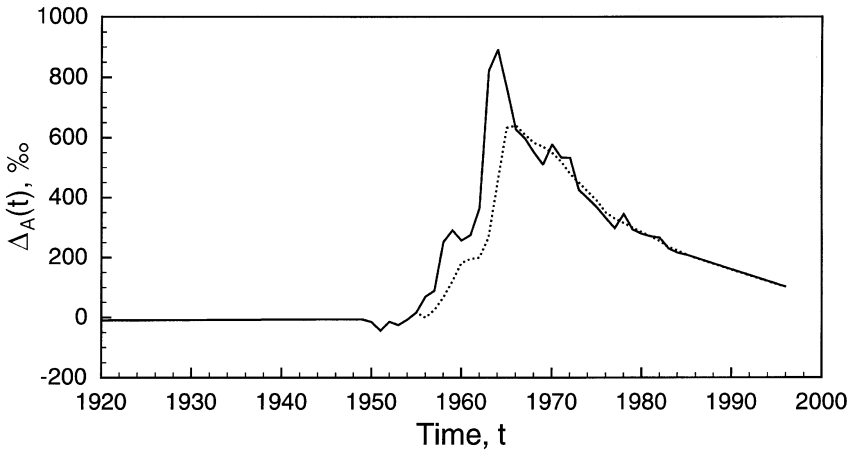

Fig. 4 Record and estimates of atmospheric Δ_A from 1920 to 1997 in the northern hemisphere (solid line) and the southern hemisphere (dotted line). All values are relative to a prebomb, age and $\delta^{13}C$ corrected standard, which, by definition, has a Δ-value of 0‰. Prebomb era data are estimated assuming a steady state prebomb atmospheric ^{14}C content and a ^{14}C half-life of 5730 years.

Levin *et al.* (1985) (S. Trumbore, pers. comm.). Southern hemisphere data up to 1993 are from the study of Manning & Melhuish (1994). 1994–97 southern hemisphere data are given the same values as the northern hemisphere (Fig. 4).

With the age correction, we calculate two parameters, the radiocarbon content of carbon respired from the terrestrial biosphere, Δ_R, and stored in the biosphere, Δ_C:

$$\Delta_R(t) = \int_0^\infty \Delta_A(t - \tau)\ \phi(\tau)\ d\tau \tag{25}$$

$$\Delta_C(t) = \int_0^\infty \Delta_A(t - \tau)\ \psi(\tau)\ d\tau. \tag{26}$$

The isotopic disequilibrium forcing coefficient of ^{14}C, ζ^{14}, as in (23), is Δ_R minus Δ_A:

$$\zeta^{14}(t) = \Delta_R(t) - \Delta_A(t)\,. \tag{27}$$

Δ_C and Δ_R can be compared against bulk soil and respiratory measurements and against measurements of individual pools within a model (but only when the pool represents a measurable quantity). ζ^{14} could be used in budgets of atmospheric ^{14}C, as for ^{13}C.

Site analysis

To demonstrate the usefulness of impulse response functions in summarizing important components of carbon turnover in different ecosystems, we perform the impulse response transformations of three cells in the CASA model in some depth. These are the same three cells analysed by Thompson *et al.* (1996) in their point analysis: a tropical forest cell centred at 2.5°S, 59.5°W, a boreal forest cell centred at 54.5°N, 66.5°W, and a grassland cell centred at 41.5°N, 99.5°W. A number of parameters, such as the mean age of stored carbon and the mean residence time, are calculated for each cell, but individual carbon pools are also analysed. Using impulse response functions for each pool in the system, we calculated for each the mean age of stored carbon, the transit or turnover time, and Δ_C (which on a pool by pool basis is the same as Δ_R).

Results and discussion

Impulse response transformation of a simple box model

$\Psi(\tau)$, $\Phi_l(\tau)$ and $\Phi_r(\tau)$ were calculated for the entire GPP- and NPP-referenced Emanuel *et al.* (1981) models (Fig. 5) as well as for each pool within the GPP-reference model (Fig. 6). Since total system losses were solely respiratory, $\Phi_l(\tau)$, $\Phi_r(\tau)$ and $d\Psi(\tau)/d\tau$ for the whole system at $\tau > 0$ were all equivalent (eqn 15). Since each pool in the model decayed exponentially, and because $\Phi_r(\tau)$ is a constant fraction of $\Phi_l(\tau)$, $\Phi_r(\tau)$, $\Phi_l(\tau)$ and $\Psi(\tau)$ were related to each other by a simple scalar.

The major differences between the NPP-and GPP-referenced models were: (i) higher $\Psi(\tau)$ for low τ (up to τ = 72 years) in the GPP-referenced model due to the fact that GPP is a larger pulse than NPP; and (ii) higher $\Psi(\tau)$ for high τ in the NPP-referenced model since plant respiration was eliminated, leaving older carbon cohorts to accumulate more carbon than their GPP counterparts. Furthermore, the change in slope of the log-y plots of $\Phi(\tau)$ and $\Psi(\tau)$ (Fig. 5) shows that turnover rates varied with age: as the carbon shifted between different reservoirs, the slope was reduced.

$\Psi(\tau)$ was calculated for each pool of the GPP-referenced model (Fig. 6; see Appendix). Shifts in pool dominance were observed as the older pools accumulated carbon at the expense of younger ones (Fig. 6), consistent with the overall decline in system decomposition rate with age (as seen in Fig. 5). The majority of the carbon over the age of 10 years was found in woody tree parts or the active soil carbon reservoir, both of which, under the Emanuel model, decay slowly and contain the majority of total system carbon storage at steady state.

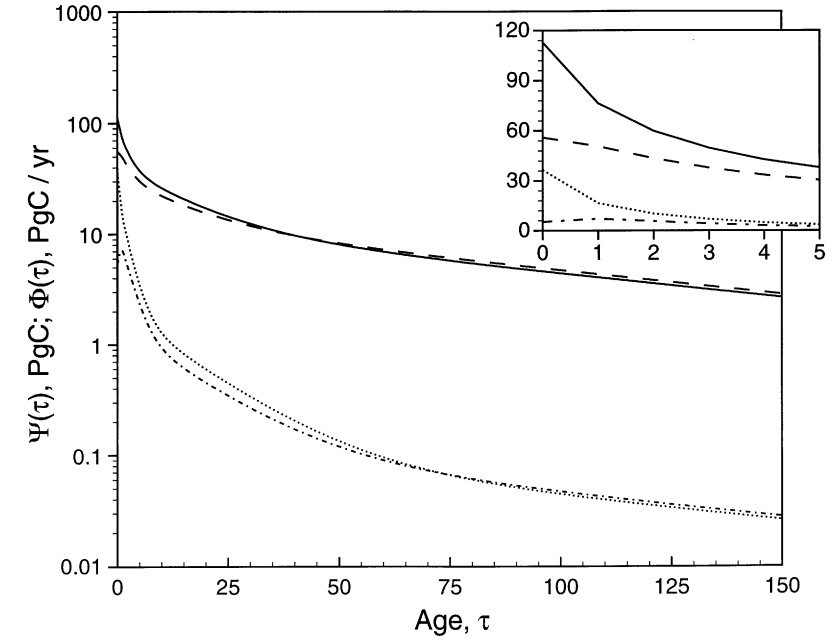

Fig. 5 Impulse response functions of GPP-and NPP-referenced versions of the five-reservoir model (Fig. 1a,b). Carbon storage $\Psi(\tau)$ and respiration $\Phi(\tau)$ following a unit pulse of carbon. The solid line is $\Psi_{GPP}(\tau)$, the dotted line is $\Phi_{GPP}(\tau)$, the long dashed line is $\Psi_{NPP}(\tau)$, and the dashed-dotted line is $\Phi_{NPP}(\tau)$. The nonconvergence between $\Psi_{GPP}(\tau)$ and $\Psi_{NPP}(\tau)$ and between $\Phi_{GPP}(\tau)$ and $\Phi_{NPP}(\tau)$ is due to small increases in the turnover time of the nontree ground vegetation and nonwoody tree parts pools with conversion to an NPP-referenced model. The insert is an expanded view of the first five years.

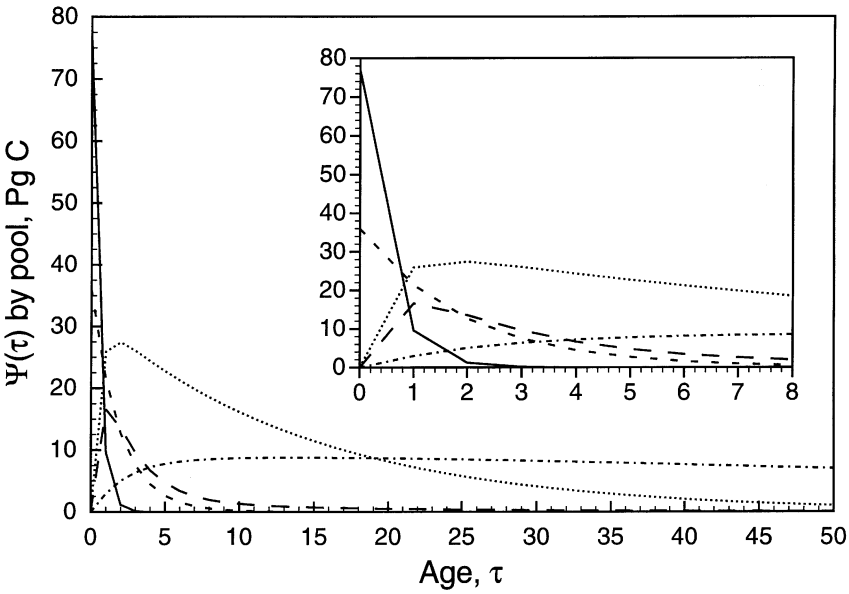

Fig. 6 $\Psi(\tau)$ for each pool of the model described in Fig. 1 (nonwoody tree parts – solid line; woody tree parts – dotted line; nontree ground vegetation – short dashed line; detritus/ decomposers – long dashed line; active soil carbon – dashed dotted line). The inset provides an expanded view of the tradeoffs during the early stages of turnover.

As mentioned previously, each pool in the model of Emanuel *et al.* (1981) decays exponentially; thus, by definition, $\phi(\tau)$ and $\psi(\tau)$ are equivalent. In fact, when any pool i is homogeneous, $\phi_i(\tau) = \psi_i(\tau)$. This has a number of important implications. First, by (3) and (6), the mean transit time and mean age of each pool will be the same (Table 2); and second, assuming there is no significant discrimination for or against carbon isotopes in the decomposition process, the carbon stored in and respired from the pool will be isotopically equivalent (eqn 23). The differences between the mean transit times of the different reservoirs (eqn 16) and their respective mean ages (eqn 17, Table 2) were the result of the additional time carbon spent in other pools before entering the pool in question ($P(\tau)$ is nonzero for $\tau > 0$ (eqn 15). Only those pools in which carbon entered directly from the atmosphere (*direct input*) possessed equivalent turnover times and mean ages.

Table 1 Abbreviations and definitions of variables in this study (equation numbers in parentheses)

Abbreviation	Definition
τ	Residence time; transit time; time between sequestration and release to atmosphere
T	Age; time since sequestration
$\overline{\tau}$	Mean residence time; mean transit time; (3)
$\overline{T}$	Mean age; (6)
τ_o	Turnover time; (7)
$\Phi(\tau)$	Steady state distribution of respired carbon with respect to transit time; impulse response function
Φ_T	Steady state input and output flux rate between the system and its surroundings; (1)
$\phi(\tau)$	Probability density function of transit times; time-dependent outflow response to an instantaneous input; weighting function describing the relative contribution of different influxes at times $(t - \tau)$ to present outflow at time t; Green's function; kernel function; normalized impulse response function; (2)
Ψ(T)	Steady state distribution of carbon in the system with respect to age; storage response function
Ψ_T	Steady state carbon storage in the system; (4)
ψ(T), $\psi(\tau)$	Probability density function of carbon storage with age; normalized storage response function; (5)
$\Phi_x(\tau)$	Impulse response function of cell x; (11)
$\Psi_x(\tau)$	Storage response function of cell x; (12)
A_x	Surface area of cell x; (11) and (12)
$\widehat{\Phi}(\tau)$	Spatially aggregated impulse response function; (11)
$\widehat{\Psi}(\tau)$	Spatially aggregated storage response function; (12)
ϕ_τ	Discretized version of $\phi(\tau)$; (13)
ψ_τ	Discretized version of $\psi(\tau)$; (13)
$P_i(\tau)$	Distribution of carbon entering pool i as a function of time since sequestration (if all carbon enters directly from the atmosphere, $P_i(\tau) = \delta(\tau)$, the Dirac-delta function); (15)
$\Phi_r(\tau)$	Steady state distribution of respiratory carbon loss from the reservoir as a function of time since sequestration; respiratory impulse response function; (14)
$\Phi_t(\tau)$	Steady state distribution of carbon leaving the reservoir via transfer to another reservoir as a function of time since sequestration; transfer impulse response function; (14)
$\Phi_l(\tau)$	Steady state distribution of all carbon leaving the reservoir (via either respiration or transfer) as a function of time since sequestration; $\Phi_l(\tau) = \Phi_r(\tau) + \Phi_t(\tau)$; (14)
GPP	Gross primary production; the rate of photosynthetic uptake of CO_2 from the atmosphere by plants
NPP	Net primary production; the difference between GPP and plant respiration
GPP-referenced	Input of carbon to system is via GPP and all carbon found in the system is GPP-derived
NPP-referenced	Input of carbon to system is via NPP and all carbon found in the system is NPP-derived
$k(\tau)$	Decay function; instantaneous first-order decay constant of carbon in the system as a function of age; (8)
$\tau_o(\tau)$	Instantaneous turnover time of carbon in the system as a function of age; the reciprocal of $k(\tau)$; (10)
P(t)	Net primary production (NPP) or gross primary production (GPP) as a function of time; (19) and (20)
R(t)	Total respiration rate of the system as a function of time; (19) and (20)
N(t)	Net carbon sequestration rate as a function of time; (20)
$\delta_A(t)$	^{13}C signature of the atmosphere as a function of time; (21)
$\varepsilon_{ab}(t)$	Fractionation of ^{13}C during photosynthesis by land plants as a function of time; (21)
$D^{13}(t)$	Terrestrial ^{13}C isodisequilibrium (or isotopic disequilibrium); (21)
$\zeta^{13}(t)$	Terrestrial ^{13}C isodisequilibrium forcing coefficient as a function of time; equivalent to $D^{13}(t)$ divided by $P(t)$ when $P(t)$ is not changing; (23)
Δ	Age and $\delta^{13}C$ corrected ^{14}C signature of a sample; (24)
A_{SN}	Activity of a radiocarbon sample corrected for ^{13}C; (24)
A_{ON}	Activity of the 1950 oxalic acid standard corrected for ^{13}C; (24)
γ	Rate constant for radioactive decay of ^{14}C; (24)
$\Delta_A(t)$	Δ-value of the atmosphere as a function of time; eqns 25, 26 and 27
Δ_R	Δ-value of respired carbon, (25)
Δ_C	Δ-value of stored carbon; (26)
$\zeta^{14}(t)$	Terrestrial ^{14}C isodisequilibrium forcing coefficient as a function of time; equivalent to $D^{14}(t)$ divided by $P(t)$ when $P(t)$ is not changing; (27)

A closer look at the age distributions of each pool (Fig. 6) suggests that some caution may in order when calculating radiocarbon ages from ^{14}C data. Although it is often assumed when calculating radiocarbon age in soils (Balesdent 1987), several of the carbon pools do not have exponentially shaped storage response functions. For an exponential distribution to be appropriate the following criteria must be reasonably met: (i) carbon

Table 2 Pool-by-pool analysis of the GPP-referenced carbon turnover model of Emanuel *et al.* (1981; Fig. 1a). Provided are the mean age $\overline{T}$, mean transit time $\overline{\tau}$, turnover time τ_o, and percentage of total carbon storage and respiration for each pool, using eqns 3, 6 and 7 and the solution to the GPP-referenced model of Emanuel *et al.* (1981) provided in Appendix A. At steady state, total carbon storage is 1760 Pg C. GPP is 113 Pg C y^{-1} (i.e. at steady state, Φ_T is 113 Pg C y^{-1})

Pool	Mean Age $\overline{T}$ (y)	Mean Residence Time $\overline{\tau}$ (y)	Turnover Time τ_o (y)	% Total Carbon Storage	% Total Respiration
Non-woody tree parts	0.4805	0.4805	0.4805	2.1	22.1
Woody tree parts	15.06	15.06	14.58	25.7	12.4
Non-tree ground vegetation	1.917	1.917	1.917	3.9	15.9
Detritus/decomposers	6.991	6.991	1.687	4.6	39.8
Active soil carbon	107.6	107.6	101.9	63.7	9.7
Entire model	72.82	15.50	15.58		

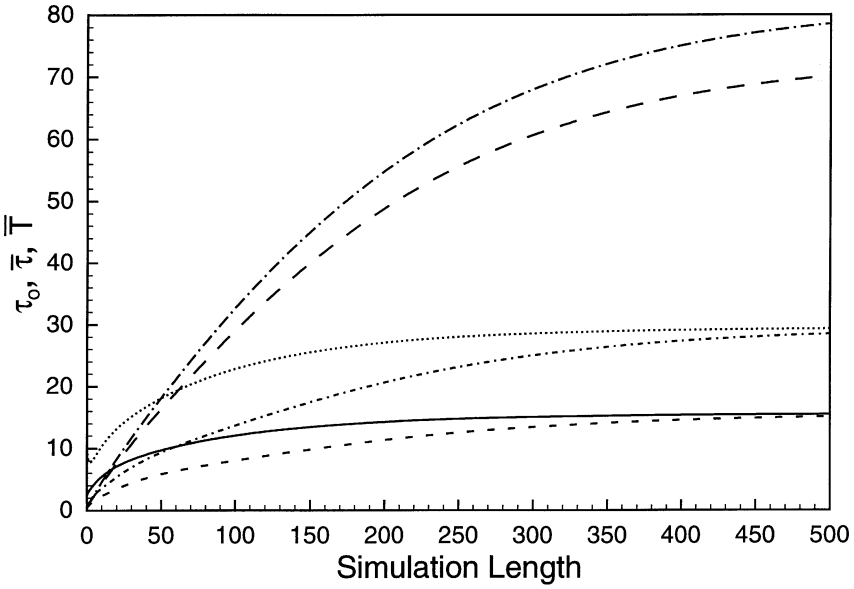

Fig. 7 Diagnostics of the model of Emanuel *et al.* (1981) as a function of simulation time. In this case, the model diagnostics are calculated not with ∞ as the upper limit of integration but with the time the simulation is run to derive the impulse and storage response functions. Presented are the turnover time (τ_o – solid line, eqn 7), mean residence time ($\overline{\tau}$ short dashed line, eqn 3), and mean age ($\overline{T}$ long dashed line, eqn 6) of the GPP-referenced version, and the turnover time (τ_o – dotted line), mean residence time ($\overline{\tau}$ short dashed dotted line), and mean age ($\overline{T}$ long dashed dotted line) of the NPP-referenced version. $\overline{\tau}$ and τ_o converge to within 1% of each other after 2000 years.

entering the different pools comes directly from the atmosphere, (ii) transfer from one soil carbon pool to another is minuscule or nonexistent (i.e. reservoirs can only accept carbon directly from the atmosphere), and (iii) the pool must decay exponentially. In addition, the meaning of terms like turnover time, mean age and mean residence time should be properly distinguished; in many cases their values may differ significantly (ex: detritus/decomposers; Table 2).

τ_o, $\overline{T}$, and $\overline{\tau}$ were calculated using (3), (6) and (7) with upper limits of integration that varied between 1 and 2000 (Fig. 7). For the GPP-referenced model, at 2000 years, τ_o was 15, $\overline{T}$ was 70 and $\overline{\tau}$ was 15 years. The differences between these numbers showed that overall the parent model did not decay exponentially, but more like the third case of Bolin & Rodhe (1973). At the end of the transformation the mean age of the NPP-referenced model was almost 10 years higher than that of the GPP-referenced model. In the NPP-referenced model, the turnover time was around 26 years but only 15 years in the GPP-referenced model. Slower turnover in the NPP-referenced model reflected the lack of plant respiration (and thus the lack of a fast initial return to the atmosphere).

Impulse response transformation of the CASA biosphere model

To illustrate this method on a spatially resolved, satellite-based NPP model, we determined the impulse response function of v1.2 of the CASA biosphere model (Figs 2 and 8,9,10). The advantage of using the globally aggregated impulse response functions $\widehat{\Phi}_\tau$ and $\widehat{\Psi}_\tau$ determined in this way is that they are equivalent to the parent model and can be used like the simpler models of Joos *et al.* (1996), Emanuel *et al.* (1981) and Moore & Braswell (1994), but still capture spatial variability in decomposition and production. Similar functions can be produced for specific geographical regions, allowing integration into larger,

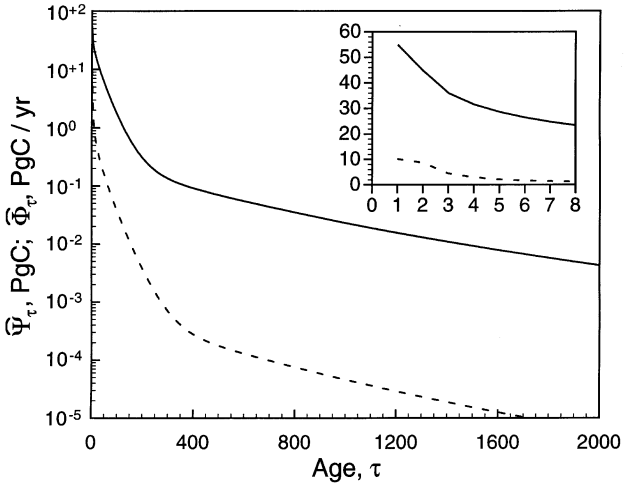

Fig. 8 Discretized, global carbon storage response Ψ_τ (solid line) and impulse response Φ_τ (dashed line) functions following a one year pulse of NPP to a standard run of the CASA model over a 2000 years simulation. The initial pulse to each cell was its own 1990 annual NPP. These results were integrated over all vegetated cells (eqns 11,12).

more complex models of the entire global carbon cycle (Bolin *et al.* 1981; Enting *et al.* 1993; Enting *et al.* 1995). Examples of regions in which we might benefit having impulse response functions are the northern forests or the tropics. We suggest this method as a new standard for the 'simple' biosphere models used in global carbon cycle studies (Joos *et al.* 1996).

The variation in $\tau_o(\tau)$ and $k(\tau)$ with cohort age for the entire globe (Fig. 9) demonstrates that carbon in the CASA model does not, taken as a whole, decompose exponentially (first-order decomposition would require constant $\tau_o(\tau)$ and $k(\tau)$ with τ). In the first two years, carbon turned over on a time-scale of 5 years; later on a time-scale of 35 years; and finally, as most of the carbon passed into the passive pool, the turnover time increased to hundreds of years. The plateauing observed here, where one pool or a group of similar pools at any given cohort age, dominates the turnover of the entire system, as has been previously observed (Schimel *et al.* 1994; McMurtrie & Comins 1996; Thompson *et al.* 1996). It has profound implications for transient studies, where the potential of a system to accrue carbon depends not only on the turnover time of the system at steady state, but also on the rate of change in production through time. Fast increases in production may lead to fast increases in respiration if turnover is rapid in the early stages of decomposition (Hungate *et al.* 1997).

The globally integrated turnover time, τ_o, of the CASA model (eqns 7, 11 and 12), was 19.4 years (Table 3). The global mean age of stored carbon $\overline{T}$ (eqn 6) and the global mean residence time of carbon $\bar{\tau}$ (eqn 3) were 71.4 years and 19.2 years, respectively. The difference between the turnover time and the mean residence time was due the limited length of the transformation (2000 years), which was not sufficient for steady state. As seen with the simple model (Fig. 7) the longer the transformation is allowed to proceed, the more these numbers converge (Bolin & Rodhe 1973).

Differences in turnover time, mean age and mean transit time of the CASA model observed as a function of latitude (Fig. 10) indicates the fact that mean age and mean transit time have different controls. At high latitudes, the mean transit time is somewhat less than the turnover time by about 10% (since convergence of the two numbers requires more time where turnover times are high, such as in cool climates). Spatial variation in turnover and mean transit time appears to be driven by vegetation class (Defries & Townshend 1994; Randerson *et al.* 1996; Thompson *et al.* 1996; Table 3), which controls the presence or absence of wood, the turnover time of live biomass, and litter chemistry. Thus, mean residence and turnover times are dependent on the initial turnover characteristics of the system. The large swath of high turnover and mean residence times across Canada and northern Eurasia corresponds to the occurrence of vegetation class 4 (needleleaf evergreen forest, Defries & Townshend 1994). Mean age, on the other hand, is correlated with the long-term storage capacity of the soil, which is controlled primarily by climate and soil texture (Parton *et al.* 1993; Schimel *et al.* 1994).

Performance of an impulse response function against its parent model

To test impulse response functions as surrogates for their parent models, as well as their ability to operate under periods of changing turnover dynamics (a condition normally prohibited by the assumptions of the method), we repeated the analysis of Thompson *et al.* (1996) using the global impulse response function determined in the previous section (Fig. 8), assuming steady-state conditions at and before the beginning of the simulation, as well as an initial global annual NPP of 48.2 Pg C y^{-1} from Thompson *et al.* (1996), using (19) and (20).

We found close agreement ($<$ 15% cumulative error) between the results from the impulse response function and the results from the Thompson *et al.* (1996) analysis (Fig. 11), but not enough agreement to justify the use of impulse response functions with these climate data sets for periods as long as 110 years. When performing analysis such as these, where it is known that climate or other factors may affect the turnover dynamics of the system, cumulative error should not be allowed to exceed 5–10%.

The change in NPP predicted by the impulse response method lacked the short-term variation seen in the work

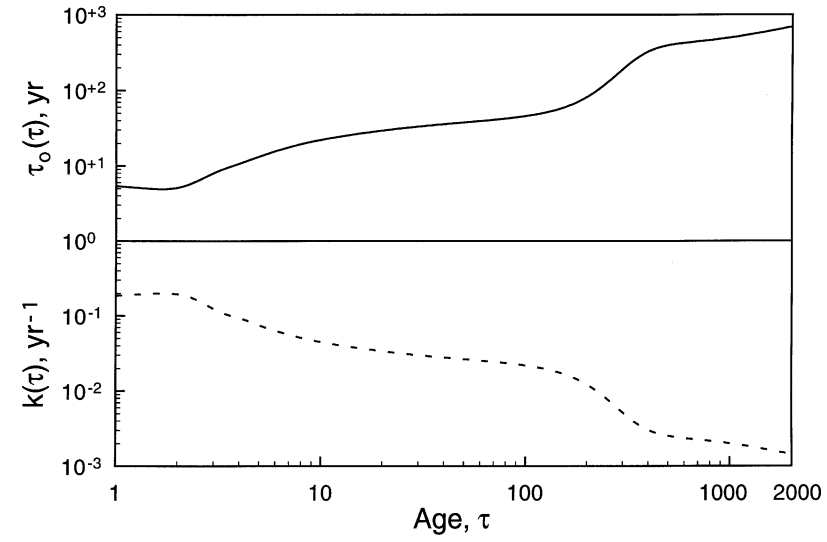

Fig. 9 The turnover time $\tau_o(\tau)$ and decay vector $k(\tau)$ of a standard 2000 years impulse response simulation of the CASA model. $k(\tau)$ (eqn 10) and $\tau_o(\tau)$ (eqn 12) are mirrored across the x-axis. $k(\tau)$ can be used as a diagnostic of the model as can $\tau_o(\tau)$.

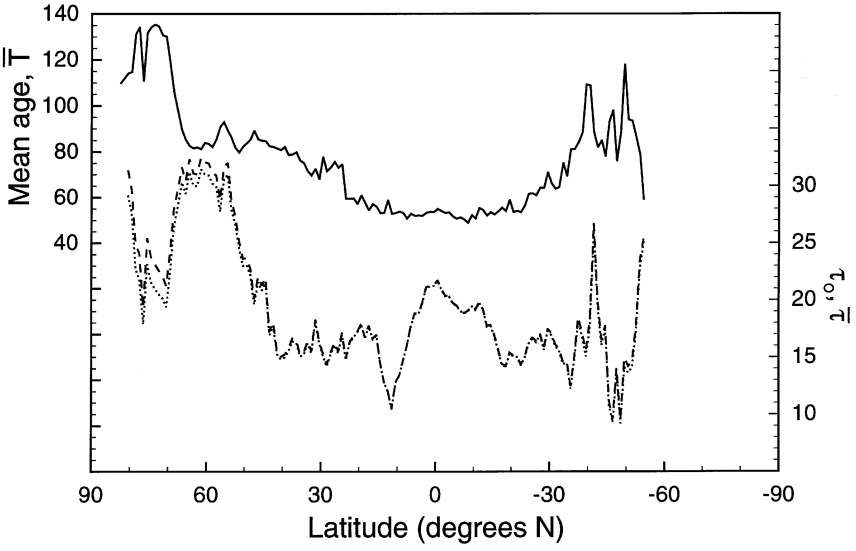

Fig. 10 The latitudinal distribution of the turnover time, τ_o (dashed line), mean age, $\overline{T}$ (solid line), and mean residence time, $\overline{\tau}$ (dotted line), of carbon in the terrestrial biosphere following a 2000 years CASA impulse response simulation (the same simulation as in Figs 8 and 9). Note the stronger latitudinal gradients in $\overline{T}$ relative to $\overline{\tau}$. Although it is hard to discern, at high latitudes $\overline{\tau}$ undershoots τ_o by as much as 10%.

of Thompson *et al.* (1996); high variation in the previous experiment was due to short-term variation in climate throughout the period, requiring high variation in NPP to match. It is uncertain that over timescales of decades this variation could be significant or even detectable given the large degree of uncertainty in the net terrestrial sink estimate. In addition, given the simplicity of this method, and the relative difficulty of the model protocol used by Thompson *et al.* (1996), limited analyses using impulse response functions over a period of a few decades are not only justifiable, but recommended. A good example of its utility would be in decadal deconvolution studies of atmospheric CO_2 and $^{13}CO_2$, where a link between terrestrial sequestration and changes in primary production could help constrain estimates of ocean and terrestrial biosphere sources and sinks.

Estimation of ^{13}C isodisequilibrium

Convolving an impulse response function, $\phi(\tau)$, against past atmospheric ^{13}C content (Fig. 2) provides an efficient means of estimating the isodisequilibrium of ^{13}C, D^{13}. We calculated the terrestrial D^{13} and ζ^{13} from 1977 to 1992 (Fig. 12) using three different impulse response functions: GPP-referenced from the Emanuel *et al.* (1981) model (Fig. 5); NPP-referenced from the Emanuel *et al.* (1981) model (Fig. 5); and NPP-referenced from the CASA model (Fig. 8). The GPP-referenced model from Emanuel *et al.* (1981) led to the highest average D^{13} (21.9 Pg C ‰ y^{-1}) for the period, and if incorporated into atmospheric ^{13}C budget analyses it would strongly shift the missing sink away from the terrestrial biosphere. The CASA model predicted the lowest average terrestrial

Table 3 Carbon storage, net primary production (NPP), mean age $\overline{T}$, mean residence time $\overline{\tau}$, and turnover time τ_o of carbon after a 2000 years pulse response simulation, summarized for each of the vegetation classes defined in Defries & Townshend (1994). Values were calculated using the impulse response method by aggregating each vegetation class into their own impulse response functions (by area-weighted averaging, (11) and (12)

Description	Number of Cells	Land Area (10^6 km^2)	Carbon Storage (PgC)	NPP (PgC y^{-1})	Mean Age $\overline{T}$ (y)	Mean Residence Time $\overline{\tau}$ (y)	Turnover Time τ_o (y)
Broadleaf evergreen trees	1095	13.4	323	14.59	54.8	22.1	22.2
Broadleaf deciduous trees	319	3.3	51	1.68	75.7	30.3	30.6
Mixed broadleaf and needleleaf trees	765	6.6	123	3.64	81.9	33.1	33.6
Needleleaf evergreen trees	2000	12.9	131	3.57	79.4	35.5	36.5
Needleleaf deciduous trees	952	5.7	50	1.67	84.4	28.8	29.9
Broadleaf trees with ground cover	1897	21.6	284	16.26	54.2	17.3	17.5
Perennial grassland	779	8.9	14	2.36	79.2	5.9	6.0
Broadleaf shrubs	1034	11.0	12	0.98	61.5	11.6	11.8
Tundra	1507	7.0	14	0.79	124.9	16.5	18.0
Hot and cold desert	1600	16.9	4	0.35	71.7	10.5	10.8
Agriculture	2608	24.7	56	9.00	90.6	6.2	6.3
Globe	14566	132.0	1062	54.9	71.4	19.2	19.4

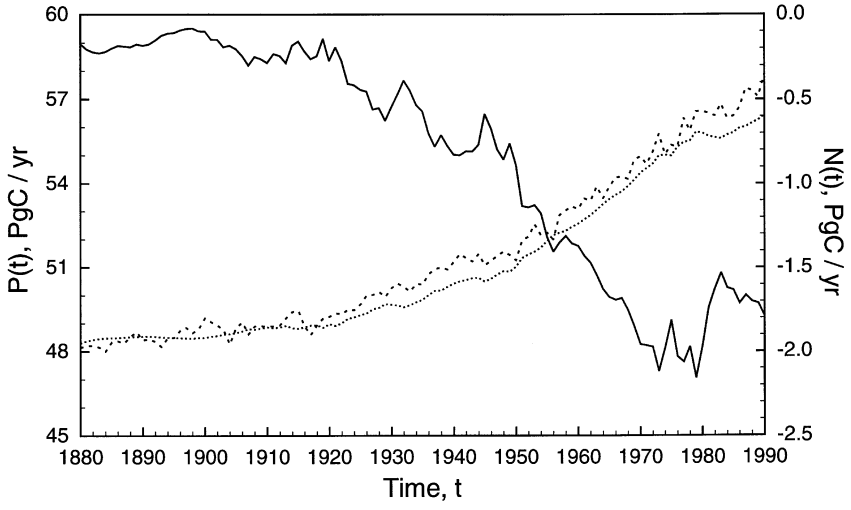

Fig. 11 Cumulative change in NPP, *P(t)* (dotted line), required to satisfy the Houghton (1995) terrestrial carbon sink estimate, *N(t)* (thick line), using the protocol detailed in Thompson *et al.* (1996) with varying climate, or using the protocol outlined in (19) and (20) and a globally aggregated impulse response function derived from the CASA model (Fig. 8). The cumulative increase in NPP predicted by the impulse response method from 1880 to 1990 undershoots the complete Thompson *et al.* (1996) model prediction by about 15%.

isodisequilibrium (16.6 Pg C ‰ y^{-1}), and if incorporated would tend to shift the sink towards the terrestrial biosphere. Variation in D^{13} for all three terms closely followed the negative rate of change in $\delta_A(t)$ (Fig. 13), where D^{13} was highest when $\delta_A(t)$ declined most rapidly. Thus, the significant year-to-year variability in these estimates was mostly due to changes in $\delta_A(t)$ at time t, rather than the long-term changes in $\delta_A(t)$ of the years before.

The highest average forcing coefficient, ζ^{13}, belonged to the NPP-referenced Emanuel model (0.33‰), while the GPP-referenced Emanuel model predicted the lowest

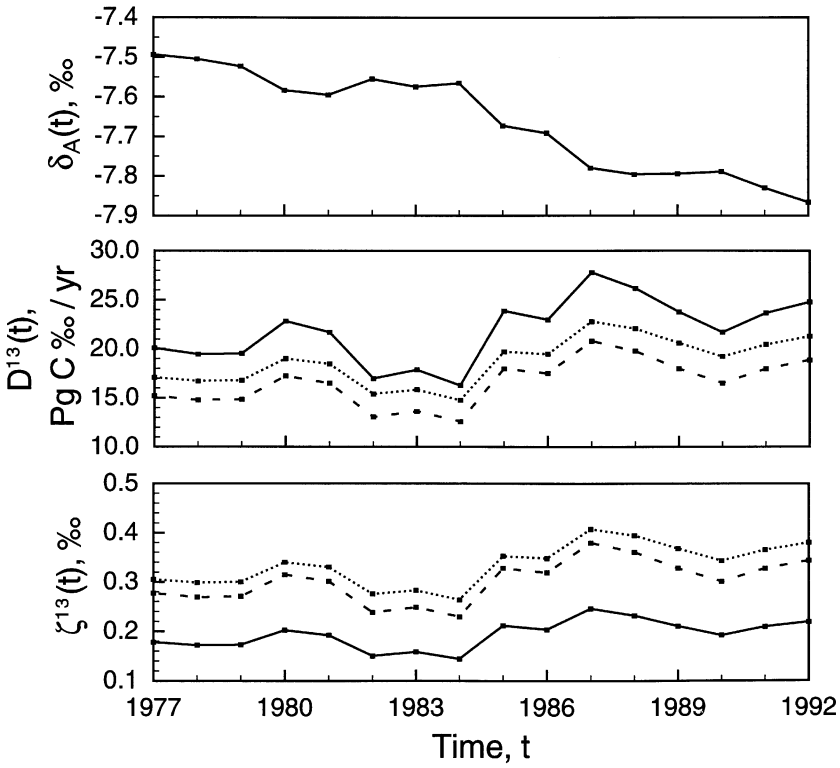

Fig. 12 Atmospheric ^{13}C data, $\delta_A(t)$ from Fig. 3 over the period from 1977 to 1992 (upper panel); estimates of $D^{13}(t)$ (Pg C‰ y^{-1}, middle panel) using the GPP-referenced model of Emanuel *et al.* (1981) (solid line), the NPP-referenced model of Emanuel *et al.* (1981) (dotted line) or the CASA model (dashed line); and estimates of terrestrial ζ^{13} (‰, lower panel) using the same models with the same key.

(0.19‰). Given the large variation observed in D^{13} and ζ^{13}, considerable care should be taken when determining what kind of model to use. Some confusion over this point has already arisen: Wittenberg & Esser (1997) assumed that the Emanuel model was NPP-referenced when they divided the isodisequilibrium (26.5 Pg C ‰ y^{-1}; from Enting *et al.* 1993[a]) by 56 Pg C y^{-1} (the approximate NPP value for the Emanuel model) to derive a forcing coefficient of 0.47‰ for 1987. Consistency requires that they calculate a GPP-referenced forcing coefficient of about 0.23‰.

It should be emphasized that the high interannual variation in the isodisequilibrium, as calculated here, may have a significant impact on analyses using atmospheric ^{13}C and CO_2 data to calculate the terrestrial and ocean sinks. D^{13} of the GPP-referenced Emanuel *et al.* (1981) model varied from as little as 17 Pg C‰ y^{-1} to as much as 28 Pg C‰ y^{-1} from 1977 to 1992. This variation is significant. Considering that the sink term of the budgetary equation (cf. Fung *et al.* 1997) is around 36 Pg C‰ y^{-1} (2 Pg C y^{-1} × 18‰), ignoring this variation could lead to a significant underestimation of the variation in the distribution of land and ocean sinks. The efficiency of impulse response function in calculating D^{13} and ζ^{13} begs that instead of just assuming an interannually stable isodisequilibrium, it would be far better to include an impulse response function in the budgetary analysis. Indeed, if included, it would also be possible to solve for interannual variation in production using (19) and (20). Further effort should be made to use impulse response functions in these sorts of analyses.

The global variation in ζ^{13} (Fig. 13), from as little as 0.1‰ to more than 0.55‰ in the northern forests, highlights the strong spatial variability found in the terrestrial biosphere with respect to rates of τ_o (Fig. 10). A globally uniform ζ^{13}, as used by Enting *et al.* (1995), should be used with caution, especially since gross fluxes of carbon covary with turnover time (Thompson *et al.* 1996). A high

[a]We were not able to reproduce the ^{13}C isodisequilibrium estimate of 26.5 Pg C ‰ y^{-1} for 1987 given by Enting *et al.* (1993). Using the piece-wise, linear $\delta^{13}C$ record that they use in their study, we attempted to reproduce their results in three different ways: (i) using their method which gave an isodisequilibrium of 22.7 Pg C ‰ y^{-1}; (ii) convolving a discrete version of Emanuel *et al.* (1981) GPP-referenced model against $\delta_A(t)$ which gave a value of 23.0 Pg C ‰ y^{-1}; and (iii) convolving an explicit integration of the Emanuel *et al.* (1981) impulse response function against the piece-wise $\delta_A(t)$ of Enting *et al.* (1993) which gave a value of 23.1 Pg C ‰ y^{-1}. However, we did find that by using their method with the last section of the piece-wise, linear $\delta^{13}C$ function changed so that it had the same slope as the previous term (the piece fom 1960 to 1980), we derived their published result (26.5 Pg C ‰ y^{-1}).

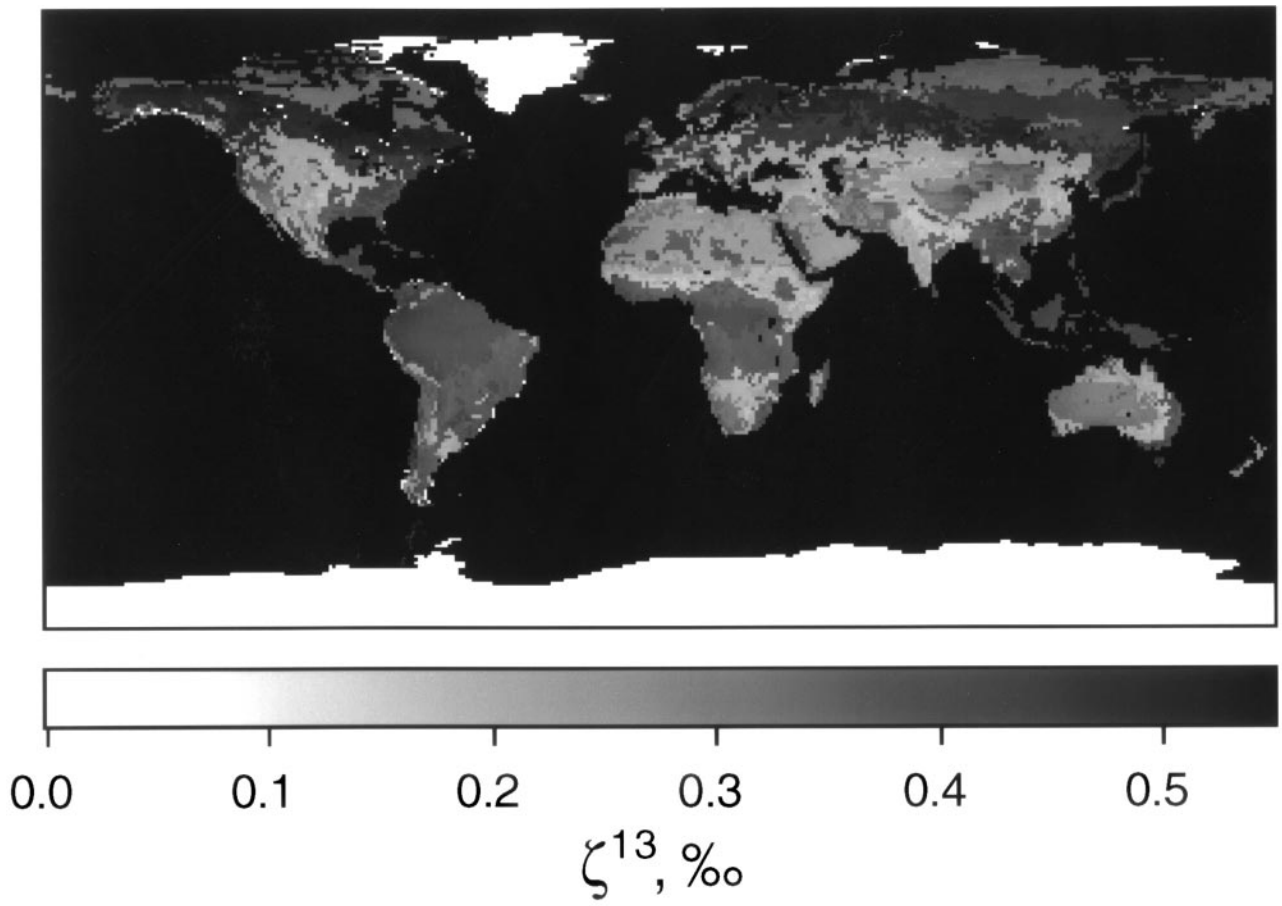

Fig. 13 The global distribution of ζ^{13} in 1992 using (23) and each cell's $\phi(\tau)$. The impulse response functions were convolved against δ_A data from Fig. 3.

ζ^{13} superimposed on a large gross flux of carbon (high NPP) will lead to a large reduction in the time-decrease in atmospheric ^{13}C within that site's footprint and reduce the global need for a strong terrestrial photosynthesis to explain trends in atmospheric $\delta^{13}C$.

Estimation of stored and respired soil ^{14}C

If the carbon stored in the terrestrial biosphere is significantly older than the carbon respired (global $\overline{T}$ – 71.4 years; global $\bar{\tau}$ – 19.2 years), then we would expect their corresponding ^{14}C ages to be quite different as well. However, a convolution of the northern hemisphere Δ_A data (Fig. 4) against Ψ_τ and Φ_τ from the CASA model (Fig. 8) indicates that these values are nearly the same: 170‰ and 175‰, respectively. The similarity is due, in this case, to the fact that $\Delta_A(t)$ does not change monotonically, but rather has a significant mode in 1964; the overlap of the two very different response functions, Ψ_τ and Φ_τ, across $\Delta_A(t)$ is such that (i) the peak is missed by the response function due to the higher probability of younger carbon being represented (as in the case of Φ_τ), or (ii) it is smoothed out due to the high probability of much older carbon being represented (as in the case of Ψ_τ). The similarity between the two values is thus largely coincidental, but it does point out an important point, that despite large differences between $\bar{\tau}$ and $\overline{T}$, representative radiocarbon ages may not be divergent.

With northern and southern hemisphere $\Delta_A(t)$ data (Fig. 4), we calculated for 1995 the spatial distribution of bulk ^{14}C content in plants and soils, or the *biospheric* Δ_C, as well as the isodisequilibrium forcing coefficient of ^{14}C, ζ^{14} (Fig. 14). The 'ghost' line along the equator of both images is due to the different Δ_A data used for the northern and southern hemisphere (Fig. 4). As far as we know, these are the first global estimates of spatially resolved Δ_C and ζ^{14}.

With impulse response functions from three different cells in the CASA model, as well as separate functions for different pools within those cells, we made explicit comparisons between modelled and observed ^{14}C signatures. Three sites were chosen for this analysis: a tropical

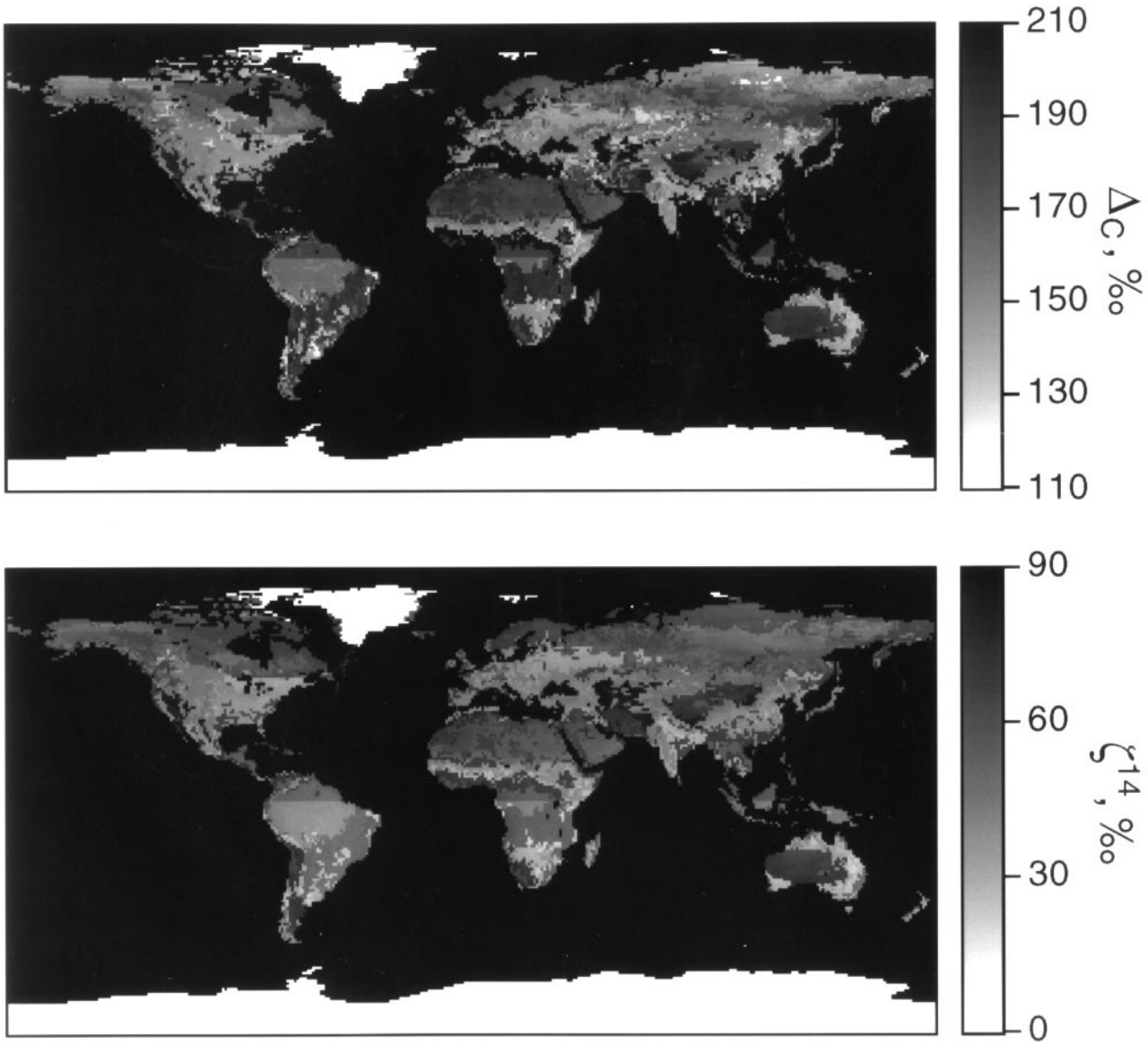

Fig. 14 The global distribution of total biospheric Δ_C values for each land point in 1995 calculated by (26) and historical Δ_A data (Fig. 4), as well as the ^{14}C forcing coefficient, ζ^{14}, calculated by (27).

wet forest site, a boreal evergreen needleleaf forest site, and a perennial grassland site. Several points (Table 4): (i) τ_0 varied by site, increasing in magnitude from the grassland site (9.83 years) to the boreal forest site (37.9 years), but $\overline{T}$ followed a different pattern, increasing from the tropical forest site (49.04 years) to the grassland site (141.5 years); (ii) the isodisequilibrium of ^{13}C increased with turnover time; and (iii) the turnover times of the different pools were typically less than their mean ages (the slow pools and microbial pools show this dramatically). Turnover time, in this case, is the time required to traverse the pool along, while mean age is the time required to traverse the entire system.

The last point demonstrates that an exponential decay assumption may not be valid when calculating the age of stored or respired carbon with radiocarbon. For example, soil inputs of above- and below-ground woody biomass in the boreal site strongly skewed the age distribution of the soil pools away from exponential (extreme example: Table 4, boreal site slow pool, $\overline{T}$ vs. τ_0). Using an exponential decay assumption in this case would lead to an overestimation of the turnover time. There may be ways around this if properly modelled. Most promising is that with more detailed impulse response analyses of regional scale models, it may be possible to deconstruct currently

Table 4 Carbon turnover statistics for three cells modelled under CASA, typical of a tropical forest (cell centred at 2.5°S, 59.5°W), a boreal forest (54.5°N, 66.5°W), and a perennial grassland (41.5°N, 99.5°W), as used in Thompson *et al.* (1996), from a 2000 years pulse response transformation. The model is NPP-referenced. The vegetation classification is by Defries & Townshend (1994) and soil texture classification is by Zobler (1986). ^{14}C and ^{13}C values are reported for 1996 using data from Figs 3 and 4. Turnover times for each pool are by (16 and mean ages are by (18)

Tropical wet forest (class 1), medium texture soil (class 4)

NPP:	1070 gC m^{-2} y^{-1}	ζ^{13}:	0.377‰	ζ^{14}:	55.9‰
ψ_T:	22 785 gC m^{-2}	*% stored in root biomass:*	2.82%	τ_o *of root biomass:*	1.8 y
τ_o:	21.32 y	*% stored in live wood:*	64.12%	τ_o *of live wood:*	41.0 y
$\overline{T}$:	49.04 y	*% stored in leaf biomass:*	2.82%	τ_o *of leaf biomass:*	1.8 y

		Surface			Soil					
	Herbivores	Metabolic	Structural	Microbial	Metabolic	Structural	Microbial	Woody debris	Slow	Passive
% total C storage	0.04%	0.11%	1.16%	0.20%	0.11%	1.47%	0.63%	8.18%	13.18%	5.16%
% total resp.	6.77%	9.72%	4.31%	9.65%	9.72%	6.21%	12.99%	16.00%	24.42%	0.22%
$\overline{T}$ (y)	1.87	2.02	4.31	24.54	1.91	3.81	21.93	46.22	29.22	299.35
τ_o (y)	0.083	0.15	2.39	0.27	0.13	2.01	0.44	5.23	6.33	279.04
ζ^{14} (‰)	119.2	120.6	143.2	148.9	119.5	138.1	173.5	169.7	196.5	–7.5

Boreal evergreen needleleaf forest (class 4), coarse/medium (organic) texture soil (class 7)

NPP:	143 gC m^{-2} y^{-1}	ζ^{13}:	0.616‰	ζ^{14}:	*78.5‰*
Ψ_T:	5421 gC m^{-2}	*% stored in root biomass:*	4.40%	τ_o *of root biomass:*	5.0 y
τ_o:	37.9 y	*% stored in live wood:*	36.9%	τ_o *of live wood:*	42.0 y
$\overline{T}$:	85.1 y	*% stored in leaf biomass:*	4.40%	τ_o *of leaf biomass:*	5.0 y

		Surface			Soil					
	Herbivores	Metabolic	Structural	Microbial	Metabolic	Structural	Microbial	Woody debris	Slow	Passive
% total C storage	0.00%	0.03%	3.25%	0.38%	0.02%	2.80%	0.86%	15.38%	24.96%	6.56%
% total resp.	0.84%	1.29%	14.75%	9.83%	0.92%	14.41%	17.22%	16.01%	24.58%	0.15%
$\overline{T}$ (y)	5.06	5.77	9.25	34.46	5.49	8.37	42.70	59.44	53.63	701.26
τ_o (y)	0.083	0.60	4.06	0.89	0.47	3.35	1.10	17.5	21.2	933.36
ζ^{14} *(‰)*	154.0	161.5	202.7	179.0	158.5	191.6	187.3	149.6	182.3	–72.5

Perennial grassland (class 7), medium texture soil (class 4)

NPP:	450 gC m^{-2} y^{-1}	ζ^{13}:	0.185‰	ζ^{14}:	58.2‰
Ψ_T:	4426 gC m^{-2}	*% stored in root biomass:*	7.63%	τ_o *of root biomass:*	1.5 y
τ_o:	9.83 y	*% stored in live wood:*	(no wood)	τ_o *of live wood:*	(no wood)
$\overline{T}$:	141.5 y	*% stored in leaf biomass:*	7.63%	τ_o *of leaf biomass:*	1.5 y

		Surface			Soil					
	Herbivores	Metabolic	Structural	Microbial	Metabolic	Structural	Microbial	Woody debris	Slow	Passive
% total C storage	0.09%	1.24%	3.84%	0.81%	0.93%	3.96%	3.15%	(no wood)	45.71%	25.00%
% total resp.	6.30%	17.93%	6.58%	9.12%	17.88%	7.82%	14.85%	(no wood)	19.28%	0.24%
$\overline{T}$ (y)	1.56	2.13	4.45	3.14	1.80	3.73	15.35	(no wood)	23.12	518.64
τ_o (y)	0.083	0.408	2.73	0.53	0.28	2.22	0.88	(no wood)	12.82	565.17
ζ^{14} *(‰)*	117.4	123.0	145.8	132.8	119.7	138.6	189.0	(no wood)	254.7	– 40.5

existing models such that they are more easily calibrated with ^{14}C data.

Uses and caveats

Impulse response functions derived from more complex carbon turnover models can be used (i) as surrogates for their parent models, (ii) as model diagnostics, or (iii) to determine the effect of the terrestrial biosphere on the global carbon cycle by convolving or deconvolving them against past changes in atmospheric or biospheric properties. It should be noted that these functions are only valid for linear systems with time-invariant dynamics; care must be taken when describing a potentially variable system

with a single impulse response function, a problem pointed out by Joos *et al.* (1996) and Lewis & Nir (1978).

A number of factors, including elevated nitrogen deposition and atmospheric CO_2, may significantly influence terrestrial carbon dynamics and are worthy of further consideration in this context. Since impulse response functions are *hysteric*, any change in their shape may render their use over the historical period somewhat questionable. As such, one set of impulse response functions can go only so far to describe the terrestrial biosphere over a certain range of conditions.

The spatially aggregated impulse response functions derived from the CASA model are useful only when the initial geographical distribution of annual NPP (derived from NDVI) as well as terrestrial carbon turnover dynamics remain constant with time. On one level, this limits the usefulness of impulse response functions in comparisons of different models. But if the comparison is a steady state comparison, impulse response functions are ideal. These globally aggregated 1D models (Fig. 8) could become standards for comparison and validation in studies of present and future global carbon turnover. They may also become valuable tools in more complex analyses of the atmospheric budget of CO_2, $^{13}CO_2$ and $^{14}CO_2$.

Impulse response functions are useful comparative tools and may nicely complement other indices of model performance. The VEMAP (1995) exercise focused on changes in production and carbon storage under changing climate and doubled-ambient atmospheric CO_2 to determine the functional differences between three biogeochemistry models, TEM, Biome-BGC and CENTURY. Since impulse response functions are far more useful as prognostic variables than the mean transit time or mean age of a system, we urge that these functions be reported in any analysis of ecosystem response to perturbation.

Impulse response functions are simple and require little CPU time. They have been used previously in descriptions of atmospheric, oceanic and terrestrial turnover (Bolin 1975), and as Joos *et al.* (1996) point out, although the interaction between different components of the global carbon cycle are sometimes nonlinear, their integrated function can be neatly described by a series of impulse response functions with explicit functions describing their interaction.

Conclusions

1 Impulse response functions facilitate diagnosis, comparison, and validation of terrestrial carbon biogeochemistry models. With them it is possible to calculate important flux-weighted parameters that are difficult to derive under complicated pool-orientated schemes. They can also be used as components of larger models describing atmosphere–ocean and atmosphere–biosphere exchange. Functions can be derived (a) for the entire globe, (b) across geographical regions or biomes (individual biomes, latitudinal zones, or individual grid cells), or (c) for individual pools or groups of pools within a larger system.

2 The impulse response function of a simple five-box biosphere model (Emanuel *et al.* 1981) demonstrated that age distributions of some fractions of soil organic matter, even if they decompose homogeneously, are not exponential. 'Downstream' pools may receive previously processed carbon from younger pools, moving the mode of their age distribution away from $\tau = 0$. An exponential age distribution may be assumed for a given carbon pool if and only if its sole source of carbon is the atmosphere and it decays exponentially.

3 The simulation time of a derived impulse response function may strongly impact the apparent turnover time, mean residence time and mean age (Fig. 7). Near steady state, mean residence times and turnover times in systems that receive all of their carbon directly from the atmosphere converge. Mean age, however, is usually larger than the mean residence or turnover time and takes longer to equilibrate.

4 Latitudinal impulse response functions of the CASA biosphere model indicate that global turnover and mean residence times are dependent on short-term turnover dynamics, while mean age is dependent on long-term dynamics. This creates different distributions of the age of stored vs. respired carbon.

5 An impulse response function from v1.2 of the CASA model performed well against the Thompson *et al.* (1996) analysis in predicting changes in NPP necessary to satisfy the terrestrial carbon over the period 1880–1990. But 15% cumulative error was observed, due largely to climate sensitivity in the full model. Given the size of the error, it may be better to restrict such analyses to periods of a few decades.

6 The high dependence of ζ^{13} and D^{13} on the model used to calculate them ($>$ 50% variation among models) suggests care must be taken when choosing the model. The isodisequilibrium is strongly dependent on recent, short-term changes in atmospheric $\delta^{13}C$. Since it is necessary to use turnover models for the isodisequilibrium, anyway, we raise the question of whether impulse response functions might be used to constrain, simultaneously, in $CO_2/^{13}C$ analyses such as those of Francey *et al.* (1995) and Ciais *et al.* (1995b), the relationship between production and the terrestrial carbon sink (eqns 19 and 20) and the relationship between turnover and the isodisequilibrium (eqn 22).

7 Bulk plant and soil ^{14}C content and ζ^{14} estimates are made for every grid cell modelled under the CASA model. The distribution of both is strongly dependent on the near-term carbon turnover dynamics of the different systems. As far as we know, this is the first global estimate of ^{14}C

isodisequilibrium. The use of ^{14}C data with this method may prove a valuable tool for model validation.

Acknowledgements

This research was supported by a WESTGEC Grant to C. B. Field and J. A. Berry at the Carnegie Institution of Washington and a NASA EOS/IDS grant to D. A. Randall and H. A. Mooney. MVT is supported by a NSF Graduate Student Fellowship. JTR was supported by a NASA Earth System Science Graduate Student Fellowship. We thank I. Y. Fung and C. B. Field for their insights during a number of valuable discussions on the global carbon cycle. We also thank M. Goulden, A. Hirsch, M. Torn, and S. Trumbore for helpful comments on earlier versions of the manuscript. Data from all figures and model code used in this study are available from the authors.

References

Amthor JS, Koch GW (1996) Biota growth factor β: stimulation of terrestrial ecosystem productivity by elevated atmospheric CO_2. In: *Carbon Dioxide and Terrestrial Ecosystems* (eds Koch GW, Mooney HA), pp. 399–414. Academic Press, San Diego, CA.

Balesdent J (1987) The turnover of soil organic fractions estimated by radiocarbon dating. *Science Total Environment*, **62,** 405–408.

Bishop JKB, Rossow WB (1991) Spatial and temporal variability of global surface solar irradiance. *Journal of Geophysical Research*, **96,** 16,839–16,858.

Bolin B (1975) A critical appraisal of models for the carbon cycle. In: *The Physical Basis of Climate and Climate Modeling*, pp. 225–235. World Meteorological Organization, International Congress of Scientific Unions, UNIPUB, NY.

Bolin B, Björkström A, Keeling CD, Bacastow R, Siegenthaler U (1981) Carbon cycle modelling. In: *Carbon Cycle Modelling* (ed. Bolin B), pp. 1–28. Wiley, New York.

Bolin B, Rodhe H (1973) A note on the concepts of age distribution and transit time in natural reservoirs. *Tellus*, **25,** 58–62.

Boyce WE, DiPrima RC (1992) *Elementary Differential Equations*. Wiley, New York, 544pp.

Burcholadze AA, Chudy M, Eristavi IV, Pagava SV, Povinec P, Sivo A, Togonidze GI (1989) Anthropogenic ^{14}C variations in atmospheric CO_2 and wines. *Radiocarbon*, **31,** 771–776.

Ciais P, Tans PP, Trolier M, White JWC, Francey RJ (1995a) A large northern hemispheric CO_2 sink indicated by the $^{13}C/^{12}C$ ratio of atmospheric CO_2. *Science*, **269,** 1098–1102.

Ciais P, Tans PP, White JWC *et al.* (1995b) Partitioning of ocean and land uptake of CO_2 as inferred by $\delta^{13}C$ measurements from the NOAA Climate Monitoring and Diagnostics Laboratory global air sampling network. *Journal of Geophysical Research*, **100,** 5051–5070.

Defries RS, Townshend JRG (1994) NDVI-derived land cover classification at a global scale. *International Journal of Remote Sensing*, **15,** 3567–3586.

Emanuel WR, Killough GEG, Olson JS (1981) Modelling the circulation of carbon in the world's terrestrial ecosystems. In: *Carbon Cycle Modelling* (ed. Bolin B), pp. 335–353. John Wiley, New York.

Emanuel WR, Killough GG, Post WM, Shugart HH (1984) Modeling terrestrial ecosystems in the global carbon cycle with shifts in carbon storage capacity by land use change. *Ecology,* **65,** 970–983.

Enting IG, Trudinger CM, Francey RJ (1995) A synthesis inversion of the concentration and $\delta^{13}C$ of atmospheric CO_2. *Tellus*, **47B,** 35–52.

Enting IG, Trudinger CM, Francey RJ, Granek H (1993) Synthesis inversion of atmospheric CO_2 using the GISS tracer transport model. *CSIRO, Australia, Division of Atmospheric Research Technical Paper*, **29,** 44pp.

Eriksson E (1971) Compartment models and reservoir theory. *Annual Review of Ecological Systematics*, **2,** 67–84.

Eriksson E, Welander P (1956) On a mathematical model of the carbon cycle in nature. *Tellus*, **8,** 155–175.

Farquhar GD, Sharkey TD (1982) Stomatal conductance and photosynthesis. *Annual Review of Plant Physiology,* **33,** 317–345.

Farquhar GD, Wong SC (1987) An empirical model of stomatal conductance. *Australian Journal of Plant Physiology,* **11,** 191–210.

Field CB, Mooney HA (1986) The photosynthesis – nitrogen relationship in wild plants. In: *On the Economy of Plant Form and Function* (ed. Givnish TJ), pp. 25–55. Cambridge University Press, Cambridge.

Field CB, Randerson JT, Malmström CM (1995) Ecosystem net primary production: combining ecology and remote sensing. *Remote Sensing and Environment*, **51,** 74–88.

Francey RJ, Tans PP, Allison CE, Enting IG, White JWC, Trolier M (1995) Changes in oceanic and terrestrial carbon uptake since 1982. *Nature*, **373,** 326–330.

Friedli H, Lötscher H, Oeschger H, Siegenthaler U, Stauffer B (1986) Ice core record of the $^{13}C/^{12}C$ ratio of atmospheric CO_2 in the past two centuries. *Nature*, **324,** 237–238.

Friedlingstein P, Fung I, Holland E, John J, Brasseur G, Erickson D, Schimel D (1995) On the contribution of CO_2 fertilization to the missing biospheric sink. *Global Biogeochemical Cycles*, **9,** 541–556.

Fung IY, Field CB, Berry JA *et al.* (1997) Carbon-13 exchanges between the atmosphere and biosphere. *Global Biogeochemical Cycles*, **11,** 507–533.

Holland EA, Braswell BH, Lamarque J-F *et al.* (1997) Variations in predicted spatial distribution of atmospheric nitrogen deposition and their impact on carbon uptake by terrestrial ecosystems. *Journal of Geophysical Research*, **102D,** 15,849–15,866.

Houghton RA (1995) Land-use change and the carbon cycle. *Global Change Biology,* **1,** 275–287.

Houghton JT, Meira Filho LG (1995) *The IPCC Report on Radiative Forcing of Climate Change*. Cambridge University Press, Cambridge, UK.

Hungate BA, Holland EA, Jackson RB, Chapin FS III, Mooney HA, Field CB (1997) The fate of carbon in grasslands under carbon dioxide enrichment. *Nature*, **388,** 576–579.

Jenkinson DS (1990) The turnover of organic carbon and nitrogen in soil. *Philosophical Transactions of the Royal Society of London B*, **329,** 361–368.

Jenkinson DS, Adams DE, Wild A (1991) Model estimates of CO_2 emissions from soil in response to global warming. *Nature*, **351,** 304–306.

Jenny H (1980) *Soil Genesis with Ecological Perspectives.* Springer-Verlag, New York, 560pp.

Joos F, Bruno M, Fink R, Siegenthaler U, Stocker TF, Le Quéré C, Sarmiento JL (1996) An efficient and accurate representation of complex oceanic and biospheric models of anthropogenic carbon uptake. *Tellus*, **48B,** 397–417.

Keeling CD (1979) The Suess effect: ^{13}carbon-^{14}carbon interrelations. *Environmental Interactions*, **2,** 229–300.

Keeling CD, Bacastrow RB, Carter AF *et al.* (1989) A three-dimensional model of atmospheric CO_2 transport based on observed winds: 1. Analysis of observational data. In: *Aspects of Climate Variability in the Pacific and the Western Americas* (ed. Peterson DH), pp. 165–236. American Geophysical Union, Washington, DC.

Kindermann J, Lüdeke MKB Badeck F-W *et al.* (1993) Structure of a global and seasonal carbon exchange model for the terrestrial biosphere: the Frankfurt biosphere model (FBM). *Water, Air and Soil Pollution*, **70,** 675–684.

Kohlmaier GH, Badeck F-W, Otto RD *et al.* (1997) The Frankfurt biosphere model – a global process-oriented model of seasonal and long-term CO_2 exchange between terrestrial ecosystems and the atmosphere. 2. Global results for potential vegetation in an assumed equilibrium state. *Climate Research*, **8,** 61–87.

Levin I, Kromer B, Schoch-Fischer H *et al.* (1985) 25 years of tropospheric ^{14}C observations in central Europe. *Radiocarbon*, **27,** 1–19.

Lewis S, Nir A (1978) On tracer theory in geophysical systems in the steady and non-steady state. Part II. Non-steady state—theoretical introduction. *Tellus*, **30,** 260–271.

Lloyd J, Farquhar GD (1996) The CO_2 dependence of photosynthesis, plant growth responses to elevated atmospheric CO_2 concentrations and their interaction with soil nutrient status. I. general principles and forest ecosystems. *Functional Ecology*, **10,** 4–32.

Los SO, Justice CO, Tucker CJ (1994) A global 1° by 1° NDVI data set for climate studies derived from the GIMMS continental NDVI data. *International Journal of Remote Sensing*, **15,** 3493–3518.

Lüdeke MKB, Badeck F-W, Otto RD *et al.* (1994) The Frankfurt biosphere model: a global process-oriented model of seasonal and long-term CO_2 exchange between terrestrial ecosystems and the atmosphere. I. Model description and illustrative results for cold deciduous and boreal forests. *Climate Research*, **4,** 116–143.

Lüdeke MKB, Dönges S, Otto RD *et al.* (1995) Responses in NPP and carbon stores of the northern biomes to a CO_2-induced climatic change, as evaluated by the Frankfurt biosphere model (FBM). *Tellus*, **47B,** 191–205.

Luo YQ, Mooney HA (1995) Long-term CO_2 stimulation of carbon influx into global terrestrial ecosystems – issues and approaches. *Journal of Biogeography*, **22,** 797–803.

Luo YQ, Sims DA, Thomas RB, Tissue DT, Ball JT (1996) Sensitivity of leaf photosynthesis to CO_2 concentration is an invariant function for C-3 plants – a test with experimental data and global applications. *Global Biogeochemical Cycles*, **10,** 209–222.

Maier-Reimer E, Hasselmann K (1987) Transport and storage in the ocean – an inorganic ocean-circulation carbon cycle model. *Climate Dynamics*, **2,** 63–90.

Malmström CM, Thompson MV, Juday GP, Los SO, Randerson JT, Field CB (1997) Interannual variation in global-scale net primary production: testing model estimates. *Global Biogeochemical Cycles*, **11,** 367–392.

Manning MR, Melhuish WH (1994) *Atmospheric $\Delta^{14}C$ Record from Wellington*. Carbon Dioxide Information Analysis Center, Oak Ridge National Laboratory, ORNL/CDIAC-65, 193–201.

McGuire AD, Melillo JM, Joyce LA, Kicklighter DW, Grace AL, Moore B, Vorosmarty CJ (1992) Interactions between carbon and nitrogen dynamics in estimating net primary productivity for potential vegetation in North America. *Global Biogeochemical Cycles*, **6,** 101–124.

McMurtrie RE, Comins HN (1996) The temporal response of forest ecosystems to doubled atmospheric CO_2 concentration. *Global Change Biology*, **2,** 49–57.

McMurtrie RE, Wang Y-P (1993) Mathematical models of the photosynthetic response of tree stands to rising carbon dioxide concentrations and temperatures. *Plant, Cell and Environment*, **16,** 1–13.

Moore B III, Bolin B (1986/1987) The oceans, carbon dioxide, and global climate change. *Oceanus*, **29,** 9–15.

Moore B III, Braswell BH (1994) The lifetime of excess atmospheric carbon dioxide. *Global Biogeochemical Cycles*, **8,** 23–38.

Nir A, Lewis S (1975) On tracer theory in geophysical systems in the steady and non-steady state. Part I. *Tellus*, **27,** 372–383.

Nydal R, Lövseth K (1996) *Carbon-14 Measurements in Atmospheric CO_2 from Northern and Southern Hemisphere Sites,* 1962–93, Carbon Dioxide Information Analysis Center, Oak Ridge National Laboratory, ORNL/CDIAC-93 NDP-057, 67pp.

Parton WJ, Scurlock JMO Ojima DS *et al.* (1993) Observations and modeling of biomass and soil organic matter dynamics for the grassland biome worldwide. *Global Biogeochemical Cycles*, **7,** 785–809.

Randerson JT, Thompson MV, Malmström CM, Field CB, Fung IY (1996) Substrate limitations for heterotrophs: implications for models that estimate the seasonal cycles of atmospheric CO_2. *Global Biogeochemical Cycles*, **10,** 585–602.

Rodhe H (1992) Modeling biogeochemical cycles. In: *Global Biogeochemical Cycles* (ed. Butcher SS), pp. 55–72. Academic Press, San Diego, CA.

Running SW (1990) Estimating terrestrial primary productivity by combining remote sensing and ecosystem simulation. In: *Remote Sensing of Biosphere Functioning* (eds Hobbs RJ, Mooney HA), pp. 65–86. Springer, New York.

Running SW, Coughlan JC (1988) A general model of forest ecosystem processes for regional applications I. hydrologic balance, canopy gas exchange and primary production processes. *Ecological Modelling*, **42,** 125–154.

Running SW, Hunt ER (1993) Generalization of a forest ecosystem process model for other biomes, BIOME-BGC, and an application for global-scale models. In: *Scaling Physiological Processes: Leaf to Globe* (eds Ehleringer JR, Field CB), pp. 141–158. Academic Press, San Diego, CA.

Sarmiento JL, Le Quéré C, Pacala SW (1995) Limiting future atmospheric carbon dioxide. *Global Biogeochemical Cycles*, **9,** 121–137.

Sarmiento JL, Orr JC, Siegenthaler U (1992) A perturbation of CO_2 uptake in an ocean general circulation model. *Journal of Geophysics Research*, **97,** 3621–3645.

Schimel DS (1995) Terrestrial ecosystems and the carbon cycle. *Global Change Biology*, **1,** 77–91.

Schimel DS, Braswell BH, Holland EA *et al.* (1994) Climatic, edaphic, and biotic controls over storage and turnover of carbon in soils. *Global Biogeochemical Cycles*, **8,** 279–294.

Schimel DS, Enting I, Heimann M, Wigley TML Raynaud D, Alves D, Siegenthaler U (1995) CO_2 and the carbon cycle. In: *IPCC WGI Report: Radiative Forcing of Climate Change* (eds Houghton JT, Meira Filho LG), Cambridge University Press, Cambridge, UK.

Shea DJ (1986) *Climatological Atlas:* 1950–79, Tech. Note NCAR TN-269+STR, National Centre for Atmospheric Research, Boulder, CO.

Siegenthaler U, Oeschger H (1978) Predicting future atmospheric carbon dioxide concentrations. *Science*, **199,** 388–395.

Siegenthaler U, Oeschger H (1987) Biospheric CO_2 emissions during the past 200 years reconstructed by deconvolution of ice core data. *Tellus*, **39B,** 140–154.

Stevenson FJ (1994) *Humus Chemistry: genesis, composition and reactions*. John Wiley, New York, 496pp.

Stuiver M, Polach H (1977) Reporting of ^{14}C data. *Radiocarbon*, **19,** 355–363.

Tans PP, Berry JA, Keeling RF (1993) Oceanic $^{13}C/^{12}C$ observations: a new window on ocean CO_2 uptake. *Global Biogeochemical Cycles*, **7,** 353–368.

Tans PP, Fung IY, Takahashi T (1990) Observational constraints on the global atmospheric CO_2 budget. *Science*, **247,** 1431–1438.

Taylor JA, Lloyd J (1992) Sources and sinks of atmospheric CO_2. *Australian Journal of Botany,* **40,** 407–418.

Thompson MV, Randerson JT, Malmström CM, Field CB (1996) Change in net primary production and heterotrophic respiration: how much is necessary to sustain the terrestrial carbon sink? *Global Biogeochemical Cycles*, **10,** 711–726.

Townsend AR, Braswell BH, Holland EA, Penner JE (1996) Spatial and temporal patterns in terrestrial carbon storage due to deposition of fossil fuel nitrogen. *Ecologica Applicata*, **6,** 806–814.

Trumbore SE (1993) Comparison of carbon dynamics in tropical and temperate soils using radiocarbon measurements. *Global Biogeochemical Cycles*, **7,** 275–290.

Trumbore SE, Davidson EA, de Camargo PB, Nepstad DC, Martinelli LA (1995) Belowground cycling of carbon in forests and pastures of Eastern Amazonia. *Global Biogeochemical Cycles*, **9,** 515–528.

VEMAP Members (1995) Vegetation/ecosystem modeling and analysis project: comparing biogeography and biogeochemistry models in a continental-scale study of terrestrial ecosystem responses to climate change and CO_2 doubling. *Global Biogeochemical Cycles*, **9,** 407–438.

Vitousek PM, Aber JD, Howarth RW *et al.* (1997a) Human alteration of the global nitrogen cycle – sources and consequences. *Ecologica Applicata*, **7,** 737–750.

Vitousek PM, Mooney HA, Lubchenco J, Melillo JM (1997b) Human domination of Earth's ecosystems. *Science*, **277,** 494–499.

Wittenberg U, Esser G (1997) Evaluation of the isotopic disequilibrium in the terrestrial biosphere by a global carbon isotope model. *Tellus*, **49B,** 263–269.

Wullschleger SD, Post WM, King AW (1995) On the potential for a CO_2 fertilization effect in forests: estimates of the biotic growth factor based on 58 controlled-exposure studies. In: *Biotic Feedbacks in the Global Climate System: will the warming feed the warming?* (eds Woodwell GM, MacKenzie FT), pp. 85–107. Oxford University Press, New York.

Zobler LA (1986) *World Soil File for Global Climate Modeling*. NASA Technical Memo, vol. 87802, 32pp.

Appendix

The Emanuel et al. *(1981) model and its impulse response function*

In this section we solve the continuous global carbon turnover model presented by Emanuel *et al.* (1981), using the differential equation solver of *Mathematica* v3.0 (Wolfram Research, Inc. Champaign, Ill. 1996). The solution is the impulse response function of the model. All calculations using these equations were carried out by analytical integration in *Mathematica*.

Emanuel *et al.* (1981) present the following system of equations for their terrestrial carbon model. This is the GPP-referenced version of the model:

$$\frac{d\boldsymbol{\Psi}_{GPP}(\tau)}{d\tau} = \begin{pmatrix} -2.081 & 0 & 0 & 0 & 0 \\ 0.8378 & -0.0686 & 0 & 0 & 0 \\ 0 & 0 & -0.5217 & 0 & 0 \\ 0.5676 & 0.0322 & 0.1739 & -0.5926 & 0 \\ 0 & 0.004425 & 0.0870 & 0.0370 & -0.009813 \end{pmatrix} \boldsymbol{\Psi}_{GPP}(\tau) + \begin{pmatrix} 77.0 \\ 0 \\ 36.0 \\ 0 \\ 0 \end{pmatrix} \boldsymbol{\delta}(T), \qquad \text{(A1)}$$

where row 1 is nonwoody tree parts, row 2 is woody tree parts, row 3 is nontree ground vegetation, row 4 is detritus/decomposers, and row 5 is active soil carbon (Fig. 1), and $\boldsymbol{\Psi}(0) = \{0, 0, 0, 0, 0\}$. The second term on the right side of the equation is the carbon pulse applied to the model at $\tau = 0$ (a Dirac delta function $\delta(\tau)$, Boyce & DiPrima (1992)).

The impulse response function of the GPP-referenced version of the Emanuel model is the solution of (A 1):

$$\boldsymbol{\Psi}_{GPP}(\tau) = \begin{pmatrix} 77.0 & 0 & 0 & 0 & 0 \\ -32.06 & 32.06 & 0 & 0 & 0 \\ 0 & 0 & 36.0 & 0 & 0 \\ -28.67 & 1.970 & 88.30 & -61.60 & 0 \\ 0.5807 & -3.653 & -12.50 & 3.911 & 11.66. \end{pmatrix} \begin{pmatrix} e^{-2.081\,\tau} \\ e^{-0.0686\,\tau} \\ e^{-0.5217\,\tau} \\ e^{-0.5926\,\tau} \\ e^{-0.009813\,\tau} \end{pmatrix}, \tau \geqslant 0\,. \quad \text{(A2)}$$

Each of these equations can be used as specific impulse response functions for each pool. The input function of the first and third pools (*per* eqn 15), $P(\tau)$, is zero for all $\tau \neq 0$, and thus receive *direct input*. The sum of the five functions provides an aggregate $\Psi(\tau)$ of (A 2):

$$\Psi_{GPP}(\tau) = 16.85\, e^{-2.081\,\tau} - 57.69\, e^{-0.5926\,\tau} + 111.8\, e^{-0.5217\,\tau} + 30.38\, e^{-0.0686\,\tau} + 11.66\, e^{-0.009813\,\tau}. \quad \text{(A3)}$$

A modified, NPP-referenced version of the model of Emanuel *et al.* (1981; Fig. 1b) was derived from the GPP-referenced models by removing the plant respiration fluxes and reducing the input from the atmosphere and other fluxes, accordingly, while maintaining as closely as possible the turnover time of each pool:

$$\frac{d\boldsymbol{\Psi}_{NPP}(\tau)}{d\tau} = \begin{pmatrix} -2.081 & 0 & 0 & 0 & 0 \\ 1.241 & -0.0686 & 0 & 0 & 0 \\ 0 & 0 & -0.5217 & 0 & 0 \\ 0.8405 & 0.06053 & 0.3477 & -0.5926 & 0 \\ 0 & 0.008068 & 0.1740 & 0.0370 & -0.009813 \end{pmatrix} \boldsymbol{\Psi}_{NPP}(\tau) + \begin{pmatrix} 38.0 \\ 0 \\ 18.0 \\ 0 \\ 0 \end{pmatrix} \delta(T). \quad \text{(A4)}$$

The solution to the NPP-referenced Emanuel model is:

$$\boldsymbol{\Psi}_{NPP}(\tau) = \begin{pmatrix} 38.0 & 0 & 0 & 0 & 0 \\ -23.43 & 23.43 & 0 & 0 & 0 \\ 0 & 0 & 18.0 & 0 & 0 \\ -20.50 & 2.706 & 88.28 & -70.48 & 0 \\ 0.4575 & -4.918 & -12.50 & 4.475 & 12.48 \end{pmatrix} \begin{pmatrix} e^{-2.081\,\tau} \\ e^{-0.0686\,\tau} \\ e^{-0.5217\,\tau} \\ e^{-0.5926\,\tau} \\ e^{-0.009813\,\tau} \end{pmatrix}, \tau \geqslant 0 \quad \text{(A5)}$$

and $\Psi_{NPP}(\tau)$ is given by:

$$\Psi_{NPP}(\tau) = -5.473\, e^{-2.081\,\tau} - 66.01\, e^{-0.5926\,\tau} + 93.78\, e^{-0.5217\,\tau} + 21.22\, e^{-0.0686\,\tau} + 12.48\, e^{-0.009813\,\tau}. \quad \text{(A6)}$$